

COVID-19 Vaccine (BNT162, PF-07302048)

BB-IND 19736

Module 2.4. Nonclinical Overview

---

## 2.4 NONCLINICAL OVERVIEW

090177e1934a5cff\Approved\Approved On: 21-Apr-2020 19:41 (GMT)

PFIZER CONFIDENTIAL

Page 1

FDA-CBER-2021-4379-0000838

## TABLE OF CONTENTS

2.4 NONCLINICAL OVERVIEW .....	1
LIST OF ABBREVIATIONS AND DEFINITION OF TERMS .....	6
2.4.1. OVERVIEW OF NONCLINICAL TESTING STRATEGY .....	8
Table 2.4.1-1. Nomenclature of the Vaccine Candidates .....	9
Table 2.4.1-2. Nonclinical Studies .....	10
2.4.2. PHARMACOLOGY .....	13
2.4.2.1. Primary Pharmacodynamics .....	13
2.4.2.1.1. Summary .....	13
2.4.2.1.2. RNA Vaccine Platforms .....	14
Figure 2.4.2-1. Overview of the Three RNA Platforms .....	14
2.4.2.1.3. Lipid Nanoparticles .....	16
Figure 2.4.2-2. Schematic Organization of a LNP .....	17
Table 2.4.2-1. Lipids in the Formulation .....	18
2.4.2.1.4. Immune Phenotype Elicited by LNP-Formulated RNA Vaccines .....	19
Table 2.4.2-2. Characteristics of the Adaptive Immune Response for the mRNA Platforms.....	19
2.4.2.1.5. SARS-CoV-2 S as a Vaccine Target .....	20
Figure 2.4.2-3. Replication Cycle of a Coronavirus .....	21
Figure 2.4.2-4. Schematic of the Organization of the SARS-CoV-2 S Glycoprotein .....	22
2.4.2.1.6. Serological and Virological Assays .....	22
2.4.2.1.7. Lack of Cell to Cell Spread of saRNA .....	23
Figure 2.4.2-5. Design of Assay to Test for saRNA Cell-to-Cell Spread .....	24
Figure 2.4.2-6. Flow Cytometry Detection of Cell Surface HA .....	24
2.4.2.1.8. In Vitro Expression of Antigens from COVID-19 vaccine RNA .....	25
Figure 2.4.2-7. Western Blot Detection of RBD and P2 S in RNA-Transfected Cells ...	25
Figure 2.4.2-8. Immunofluorescence Detection of RBD and P2 S in RNA Transfected Cells.....	26
2.4.2.1.9. Supportive Mouse Immunogenicity Studies .....	27
Figure 2.4.2-9. Influenza HA Binding and Virus Neutralization Elicited by Immunization of Mice with modRNA Encoding HA in the Clinical LNP Formulation..	27
Figure 2.4.2-10. CD4+ and CD8+ T Cell Response to LNP-Formulated modRNA Encoding Influenza HA by IFN- ELISpot.....	28

COVID-19 Vaccine (BNT162, PF-07302048)

BB-IND 19736

Module 2.4. Nonclinical Overview

Figure 2.4.2-11. IgG Response Recognizing S1 and RBD 7, 14, 21, and 28 d after Immunization with uRNA Encoding P2 S V8.....	29
Figure 2.4.2-12. Kinetics of the IgG Response Recognizing S1 and RBD after Immunization with uRNA Encoding P2 S V8.....	30
Figure 2.4.2-13. Pseudovirus Neutralization 14, 21 and 28 d after Immunization with uRNA Encoding P2 S V8.....	31
Figure 2.4.2-14. IgG Response Recognizing S1 and RBD 7, 14 and 21 d after Immunization with saRNA Encoding RBD V5.....	32
Figure 2.4.2-15. Pseudovirus Neutralization 14 d after Immunization with saRNA Encoding the RBD V5.....	33
Figure 2.4.2-16. IgG Response Recognizing S1 and RBD IgG 7, 14 and 21 d after Immunization with modRNA Encoding P2 S V8.....	34
Figure 2.4.2-17. Pseudovirus Neutralization 14 d after Immunization with modRNA Encoding P2 S V8.....	35
2.4.2.1.10. Mouse Immunogenicity Studies for COVID-19 Vaccine Candidates .....	35
Table 2.4.2-3. Design of Mouse Immunogenicity Studies for COVID-19 Vaccine Candidates.....	35
Figure 2.4.2-18. IgG Response Recognizing S1 and RBD 7, 14, 21 and 28 d after Immunization with uRNA Encoding RBD V5.....	37
Figure 2.4.2-19. Kinetics of the IgG Response Recognizing S1 and RBD after Immunization with uRNA Encoding RBD V5.....	38
Figure 2.4.2-20. Pseudovirus Neutralization Titers 7, 14, and 21 after Immunization with uRNA Encoding RBD V5.....	39
Figure 2.4.2-21. IgG Response Recognizing S1 and RBD 7, 14, 21 and 28 d after Immunization with modRNA Encoding RBD V5.....	40
Figure 2.4.2-22. Kinetics of the IgG Response Recognizing S1 and RBD after Immunization with modRNA Encoding RBD V5.....	41
Figure 2.4.2-23. Pseudovirus Neutralization 14, 21 and 28 d after Immunization with modRNA Encoding RBD V5.....	42
Figure 2.4.2-24. IgG Response Recognizing S1 and RBD 7 and 14 d after Immunization with modRNA Encoding P2 S V9.....	43
Figure 2.4.2-25. IgG Response Recognizing S1 and RBD 7, 14 and 21 d after Immunization with saRNA Encoding P2 S V9.....	44
Figure 2.4.2-26. Pseudovirus Neutralization 14 and 21 d after Immunization with saRNA Encoding P2 S V9.....	45
2.4.2.1.11. Immunogenicity Testing After Weekly Immunization of Rats in the GLP Compliant Repeat Dose Toxicology Study.....	45
Figure 2.4.2-27. IgG Responses Recognizing S1 after Repeated Immunization in the Rat Toxicology Study.....	46

090177e1934a5cffApproved\Approved On: 21-Apr-2020 19:41 (GMT)

COVID-19 Vaccine (BNT162, PF-07302048)

BB-IND 19736

Module 2.4. Nonclinical Overview

Figure 2.4.2-28. IgG Responses Recognizing RBD after Repeated Immunization in the Rat Toxicology Study.....	47
Table 2.4.2-4. IgG Concentrations Against S1 and RBD in Immunized Wistar Han Rats.....	47
Figure 2.4.2-29. Pseudovirus Neutralization Activity (pVN50) in Repeatedly Dosed Rats.....	48
2.4.2.1.12. Secondary pharmacodynamics .....	48
2.4.2.1.13. Safety pharmacology .....	48
2.4.2.1.14. Nonclinical pharmacology - Conclusions .....	48
2.4.3. PHARMACOKINETICS .....	50
2.4.3.1. Brief Summary .....	50
2.4.3.2. Methods of Analysis .....	50
2.4.3.3. In Vitro Absorption .....	50
2.4.3.4. Pharmacokinetics .....	50
2.4.3.5. Distribution .....	50
Figure 1. Bioluminescence Emission in BALB/c Mice after IM Injection of an LNP Formulation of modRNA Encoding Luciferase.....	51
2.4.3.6. Metabolism .....	51
2.4.3.7. Excretion .....	52
2.4.3.8. Pharmacokinetic Drug Interactions .....	52
2.4.4. TOXICOLOGY .....	53
2.4.4.1. Brief Summary .....	53
Table 2.4.4-1. Overview of Toxicity Testing Program .....	54
2.4.4.2. Single-Dose Toxicity .....	55
2.4.4.3. Repeat-Dose Toxicity .....	55
2.4.4.3.1. Repeat-Dose Toxicity Study of Three LNP-Formulated RNA Platforms Encoding for Viral Proteins by Repeated Intramuscular Administration to Wistar Han Rats.....	55
2.4.4.4. Genotoxicity .....	58
2.4.4.5. Carcinogenicity .....	59
2.4.4.6. Reproductive and Developmental Toxicity .....	59
2.4.4.7. Local Tolerance .....	59
2.4.4.8. Other Toxicity Studies .....	59
2.4.4.8.1. Phototoxicity .....	59

090177e1934a5cff\Approved\Approved On: 21-Apr-2020 19:41 (GMT)

PFIZER CONFIDENTIAL

Page 4

FDA-CBER-2021-4379-0000841

COVID-19 Vaccine (BNT162, PF-07302048)

BB-IND 19736

Module 2.4. Nonclinical Overview

---

2.4.4.8.2. Antigenicity .....	59
2.4.4.8.3. Immunotoxicity .....	59
2.4.4.8.4. Mechanistic Studies .....	59
2.4.4.8.5. Dependence .....	60
2.4.4.8.6. Studies on Metabolites .....	60
2.4.4.8.7. Studies on Impurities .....	60
2.4.4.8.8. Other Studies .....	60
2.4.4.9. Target Organ Toxicity .....	60
IN-TEXT TABLES AND FIGURES .....	54
Table 2.4.4-1. Overview of Toxicity Testing Program .....	54
2.4.5. INTEGRATED OVERVIEW AND CONCLUSIONS .....	61
2.4.6. LIST OF LITERATURE REFERENCES .....	63

090177e1934a5cff\Approved\Approved On: 21-Apr-2020 19:41 (GMT)

**LIST OF ABBREVIATIONS AND DEFINITION OF TERMS**

ADCC	Antibody-dependent cellular cytotoxicity
aPTT	Activated partial thromboplastin time
CAS	Chemical abstracts service
CBER	Center for Biologics Evaluation and Research
CD	Cluster of differentiation
CoV	Coronavirus
COVID-19	Coronavirus Disease 2019
DDI	Drug drug interaction
dLIA	Direct binding Luminex immunoassay
DNA	Deoxyribonucleic acid
DSPC	1,2-distearoyl-sn-glycero-3-phosphocholine
ELISA	Enzyme-linked immunosorbent assay
ELISpot	Enzyme-linked immunosorbent spot assay
FIH	First-In-Human
GGT	Gamma-glutamyl transferase
GLP	Good Laboratory Practice
HA	Hemagglutinin
HAI	Hemagglutinin inhibition assay
HEK	Human embryonic kidney
IB	Investigator's Brochure
IFN	Interferon
IgG	Immunoglobulin G
IL	Interleukin
IM	Intramuscular(ly)
IND	Investigational New Drug Application
IV	Intravenous(ly)
kDa	Kilodalton
LLOQ	Lower limit of quantification
LNP	Lipid-nanoparticle
Luc	Luciferase (from firefly <i>Pyroactomena lucifera</i> )
LUC	Large unstained cells
MERS	Middle East respiratory syndrome
modRNA	Nucleoside-modified mRNA
mRNA	Messenger RNA
NHP	Nonhuman primate
NVA	Non-vaccine antigen
OECD	Organisation for Economic Co-operation and Development
ORF	Open reading frame
P2 S	Spike protein P2 mutant
PK	Pharmacokinetics
PT	Prothrombin time
pVNT	Pseudotype virus neutralization assay

090177e1934a5cff\Approved\Approved On: 21-Apr-2020 19:41 (GMT)

COVID-19 Vaccine (BNT162, PF-07302048)

BB-IND 19736

Module 2.4. Nonclinical Overview

QC	Quality control review
QW	Once weekly
RBD	Receptor binding domain
RdRp	RNA-dependent RNA-polymerase
RNA	Ribonucleic acid
RT-PCR	Reverse transcription-polymerase chain reaction
S	SARS-CoV-2 spike glycoprotein
saRNA	Self-amplifying RNA
SARS	Severe Acute Respiratory Syndrome
SARS-CoV-2	Severe acute respiratory syndrome coronavirus 2; coronavirus causing COVID-19
SDS-PAGE	Sodium dodecyl sulfate-polyacrylamide gel electrophoresis
SEM	Standard error of the mean
siRNA	Small interfering RNA
Tfh	T follicular helper cell
Th1	Type 1 T helper cells
Th2	Type 2 T helper cells
TK	Toxicokinetic
TLR	Toll-like receptor
TNF	Tumor necrosis factor
ULOQ	Upper limit of quantification
uRNA	Unmodified mRNA
UTR	Untranslated region
V5	Variant 5; RBD
V8	Variant 8; P2 S
V9	Variant 9; P2 S
VEE	Venezuelan equine encephalitis virus
VLVs	Virus-like vesicles
VSV	Vesicular stomatitis virus
WHO	World Health Organization

090177e1934a5cff\Approved\Approved On: 21-Apr-2020 19:41 (GMT)

### 2.4.1. OVERVIEW OF NONCLINICAL TESTING STRATEGY

BioNTech and Pfizer are developing an investigational vaccine intended to prevent COVID-19, which is caused by SARS-CoV-2. The vaccine is referred to as COVID-19 vaccine (BioNTech code number BNT162; Pfizer reference number PF-07302048).

Each candidate for the vaccine contains RNA from one of three platforms:

- unmodified mRNA (uRNA)
- nucleoside modified mRNA (modRNA)
- self-amplifying RNA (saRNA)

The RNA is formulated in LNPs. Each of the RNAs expresses one of two antigens, which are based on SARS-CoV-2 spike glycoprotein (S):

- A trimerized receptor binding domain (RBD; [Kirchdoerfer et al, 2018](#)).
- The full-length, membrane-anchored glycoprotein with two introduced proline mutations (P2 S; [Pallesen et al, 2017](#); [Wrapp et al, 2020](#)).

The antigens have variants (V5 for the RBD and V8 or V9 for P2 S). Variants of the same antigen have the same amino acid sequence, but the RNAs that encode them differ in their codon optimization.

In the phase 1/2 clinical study, C4591001, four COVID-19 vaccine candidates will be evaluated:

- BNT162a1 (RBL063.3) - uRNA encoding RBD V5
- BNT162b1 (RBP020.3) - modRNA encoding RBD V5
- BNT162b2 (RBP020.2) - modRNA encoding P2 S V9
- BNT162c2 (RBS004.2) - saRNA encoding P2 S V9

Reference information on these clinical vaccine candidates and other constructs tested nonclinically is provided in [Table 2.4.1-1](#).

The primary pharmacology of the COVID-19 vaccine candidates and constructs expressing alternative antigens on the same vaccine platforms were evaluated in non-clinical pharmacology studies *in vitro* and *in vivo* ([Table 2.4.1-2](#)). *In vitro* testing demonstrated that saRNA does not spread from cell to cell ([Section 2.4.2.1.7](#)). Expression of the RBD and P2 S antigens from vaccine candidate RNAs was demonstrated in cultured cells ([Section 2.4.2.1.8](#)).

Platform properties that support the COVID-19 vaccines were demonstrated with non-SARS-CoV-2 antigens. Non-GLP *in vivo* testing of LNP-formulated modRNA encoding luciferase



examined biodistribution in BALB/c mice after IM injection ([Section 2.4.3.5](#)). A murine immunogenicity study of an LNP-formulated modRNA expressing influenza HA provided platform data against a target for which there are well-established immunogenicity benchmarks and data on cell-mediated responses ([Section 2.4.2.1.9.1](#)).

A series of mouse immunogenicity studies demonstrated that the vaccine candidates ([Section 2.4.2.1.10](#)) and additional constructs ([Section 2.4.2.1.9](#)) that are being tested in the GLP repeat-dose toxicity study rapidly elicit SARS-CoV-2 S antigen binding IgG and serum SARS-CoV-2 pseudovirus neutralizing responses. The mouse immunogenicity studies are in progress, and final study reports will be provided to the IND as they become available and prior to testing of the vaccine candidates in the Phase 1/2 trial. Immunogenicity data are also available from serum drawn 2 days after two or three weekly doses of vaccine candidates in the rat GLP repeat dose toxicity study ([Section 2.4.2.1.11](#)).

**Table 2.4.1-1. Nomenclature of the Vaccine Candidates**

Product Code	RNA Platform	Antigen Variant	Description/Translated Protein	Variant Code	GLP Tox Data	Phase 1/2 Candidate
PF-07302048	NA	NA	Pfizer code for any COVID-19 vaccine	NA	NA	NA
BNT-162	NA	NA	BioNTech code for any COVID-19 vaccine	NA	NA	NA
BNT162a1	uRNA	V5	RBD	RBL063.3	Yes	Yes
BNT162a2	uRNA	V8 <sup>a</sup>	P2 S	RBL063.1	No	No
BNT162b1	modRNA	V5	RBD	RBP020.3	Yes	Yes
BNT162b2	modRNA	V8	P2 S	RBP020.1	Yes	No
BNT162b2	modRNA	V9	P2 S	RBP020.2	No	Yes
BNT162c1	saRNA	V5	RBD	RBS004.3	Yes	No
BNT162c2	saRNA	V9	P2 S	RBS004.2	No	Yes

a. The V8 and V9 variants of the P2 S antigen have the same amino acid sequence. Different codon optimizations were used for their coding sequences.

In the mouse and rat immunogenicity studies of the vaccine candidates, antigen binding IgG responses are tested by an ELISA and functional antibody responses are tested by a SARS-CoV-2 pVNT. The serology assays are described in [Section 2.4.2.1.6](#).

A nonhuman primate immunogenicity study has been initiated to assess antigen-binding antibody, infectious SARS-CoV-2 neutralization, and Th1/Th2 T helper cell phenotypes elicited by the vaccine candidates in a species with immune responses more predictive of human responses. However, there are abundant data with non-COVID-19 vaccine candidates demonstrating that RNA platforms skew the immune response to a Th1 profile. Those data are summarized in [Section 2.4.2.1.4](#).

The potential toxicity of LNP-formulated uRNA, modRNA, and saRNA vaccine candidates encoding SARS-CoV-2 antigens administered IM is currently being studied in a GLP-compliant (pivotal) repeat-dose toxicity study in rats ([Study 38166](#)), which started dosing on 17 March 2020. The study design is described in [Section 2.4.4](#) and is based on WHO guidelines for vaccine development ([WHO, 2005](#)). Interim data from the dosing phase

of the toxicity study are provided as part of the IND in support of FIH clinical studies, as agreed upon with CBER (Advice of April 6, 2020 in response to Pre-IND meeting request PS005569). The interim report will include all dosing phase mortality, clinical observations, body weight, food consumption, body temperature, injection site dermal scores, ophthalmoscopic and auditory endpoints, hematology, coagulation, clinical chemistry, urinalysis parameters, a subset of cytokine endpoints, serology, macroscopic findings and organ weights from the dosing phase animals. Remaining cytokine results and microscopic pathology from the dosing phase as well as all the recovery phase endpoints will be submitted in a final report as soon as it becomes available, but no later than 120 days after filing the IND.

**Table 2.4.1-2. Nonclinical Studies**

Study Number	Study Type	Species / Test System	Test Item	Dose [µg]	Results	Cross reference
BNT162 vaccine studies						
R-20-0074	In vitro antigen expression and localization	HEK293T cells	BNT162a1 (RBL063.3) BNT162b1 (RBP020.3) BNT162b2 (RBP020.1) BNT162c1 (RBS004.3)	2.5	All tested items expressed the encoded S protein derived antigen.	<a href="#">Section 2.4.2.1.8</a>
R-20-0040	In vivo immunogenicity	Mice <sup>a</sup>	BNT162a1 (RBL063.3)	1, 5, 10	Immunogenicity was shown in all tested doses.	<a href="#">Section 2.4.2.1.10.1</a>
R-20-0042	In vivo immunogenicity	Mice	BNT162b1 (RBP020.3)	0.2, 1, 5	Immunogenicity was shown in all tested doses.	<a href="#">Section 2.4.2.1.10.2</a>
R-20-0085	In vivo immunogenicity	Mice	BNT162b2 (RBP020.2)	0.2, 1, 5	Immunogenicity was shown in all tested doses.	<a href="#">Section 2.4.2.1.10.3</a>
R-20-0053	In vivo immunogenicity	Mice	BNT162c2 (RBS004.2)	0.2, 1, 5	Immunogenicity was shown in all tested doses.	<a href="#">Section 2.4.2.1.10.4</a>
Supportive studies						
R-20-0073	In vivo immunogenicity	Mice	modRNA encoding influenza HA	1	HA delivered by LNP-formulated modRNA induced a strong antibody and antigen-specific T cell response.	<a href="#">Section 2.4.2.1.9.1</a>

**Table 2.4.1-2. Nonclinical Studies - Continued**

Study Number	Study Type	Species / Test System	Test Item	Dose [µg]	Results	Cross reference
R-20-0052	In vivo immunogenicity	Mice	BNT162a2 (RBL063.1)	1, 5, 10	Immunogenicity was shown in all tested doses.	<a href="#">Section 2.4.2.1.9.2</a>
R-20-0041	In vivo immunogenicity	Mice	BNT162c1 (RBS004.3)	0.2, 1, 5	Immunogenicity was shown in all tested doses.	<a href="#">Section 2.4.2.1.9.3</a>
R-20-0054	In vivo immunogenicity	Mice	BNT162b2 (RBP020.1)	0.2, 1, 5	Immunogenicity was shown in all tested doses.	<a href="#">Section 2.4.2.1.9.4</a>
R-20-0072	In vivo distribution	Mice	modRNA encoding luciferase	2	ModRNA expressed luciferase in mice with distribution in the muscle (injection site) and liver.	<a href="#">Section 2.4.3.5</a>

a. All murine testing was conducted in BALB/c mice.

After initiation of GLP repeat-dose toxicity testing of the vaccine candidates, the antigen expression and mouse immunogenicity data presented here ([Section 2.4.2.1.8](#) and [Section 2.4.2.1.10](#)) were obtained. These data led to a re-evaluation of which vaccine candidates would be chosen for clinical testing in study C4591001. Two changes were made:

1. Based on higher expression levels, BNT162b2 (RBP020.2), a modRNA that expresses P2 S V9, was chosen for clinical testing in place of the BNT162b2 (RBP020.1), a modRNA that expresses P2 S V8 and is being tested in the GLP repeat dose toxicology study. Antigens P2 S V8 and P2 S V9 have the same amino acid sequence and differ only in codon optimization.
2. Based on greater immunogenicity in mice, BNT162c2 (RBS004.2), a saRNA that expresses P2 S V9, was chosen for clinical testing in place of BNT162c1 (RBS004.3), a saRNA that expresses RBD V5 and is being tested in the repeat dose GLP toxicity study. Both the saRNA platform and the expressed antigen of the clinical candidate BNT162c2 (RBS004.2) are being tested in the repeat dose toxicology study, though in different platform-antigen combinations.

These changes are considered minor and are not expected to have a safety impact; therefore, BioNTech/Pfizer do not plan to conduct additional toxicity studies to support clinical administration. For more details see [Section 2.4.5](#).

IM administration was chosen for the toxicity study as this is the intended route of administration in the clinic. Rats were chosen for toxicity assessments as they are a commonly used rodent species for the evaluation of toxicity and they mount an immune response to vaccination with the COVID-19 vaccine candidates.

The pivotal repeat-dose toxicity study in rats was conducted in accordance with Good Laboratory Practice for Nonclinical Laboratory Studies, Code of US Federal Regulations (21 CFR Part 58), in an OECD Mutual Acceptance of Data member state. The location of records for inspection will be included in the final study report.

## 2.4.2. PHARMACOLOGY

### 2.4.2.1. Primary Pharmacodynamics

#### 2.4.2.1.1. Summary

There is an urgent need for the development of a new prophylactic vaccine given the threat posed by the increasing number of globally distributed outbreaks of SARS-CoV-2 infection and its associated disease, COVID-19. There are currently no approved vaccines or antiviral drugs to prevent or treat infection with SARS-CoV-2 or its associated disease, COVID-19 ([Habibzadeh and Stoneman, 2020](#)). RNA-based vaccines encode a viral antigen that is translated by the vaccinated organism into protein to induce a protective immune response. There are three RNA platforms under development: unmodified mRNA (uRNA), nucleoside modified mRNA (modRNA), and self-amplifying mRNA (saRNA).

More than a dozen nonclinical good laboratory practice (GLP) safety studies and clinical safety data are available for uRNA and modRNA. These data have been obtained primarily with RNAs formulated with liposomes and LNPs that are related, but not identical, to those that will be used in the planned clinical trial C4591001.

The overall nonclinical toxicity data generated by BioNTech on their portfolio suggest a favorable safety profile for uRNA, modRNA, and saRNA formulated with different nanoparticles for various administration routes including for intravenous (IV) injection. The favorable safety profile after IV dosing is notable because IV injection results in a higher systemic exposure than the intramuscular (IM) injection planned in clinical trial C4591001. Overall, the findings were mild and mostly related to the mode-of-action and the RNA-intrinsic stimulation of innate immune sensors. No unsuspected target organs of toxicity were identified. The nonclinical safety profile of uRNA and modRNA in rodents was predictive of clinical safety.

The available interim nonclinical safety and toxicity data generated in a GLP-compliant repeat-dose toxicity study of the COVID-19 family of LNP-enveloped uRNA, modRNA, and saRNA vaccine platforms encoding SARS-CoV-2 antigens are included in this IND ([Section 2.4.4.3](#)) together with other preclinical data supporting the clinical use of the COVID-19 vaccine candidates. Given the urgency of this pandemic, additional data will be submitted to the IND at the times agreed upon with CBER.

There are currently no data available on the effects of any of the COVID-19 candidates in humans. However, a number of human studies for other RNA candidate vaccines seeking different indications have provided relevant data to support RNA as a vaccine platform and thus support the COVID-19 vaccine candidates. These data have shown that certain aspects of the immune responses to RNA translate well from animals to humans and are discussed in the Clinical Overview ([Section 2.5.1.8](#)).

The safety and immunogenicity of four COVID-19 vaccine candidates (BNT162a1/RBL063.3, BNT162b1/RBP020.3, BNT162b2/RBP020.2, and BNT162c2/RBS004.2) against SARS-CoV-2 will be investigated clinically, as part of a

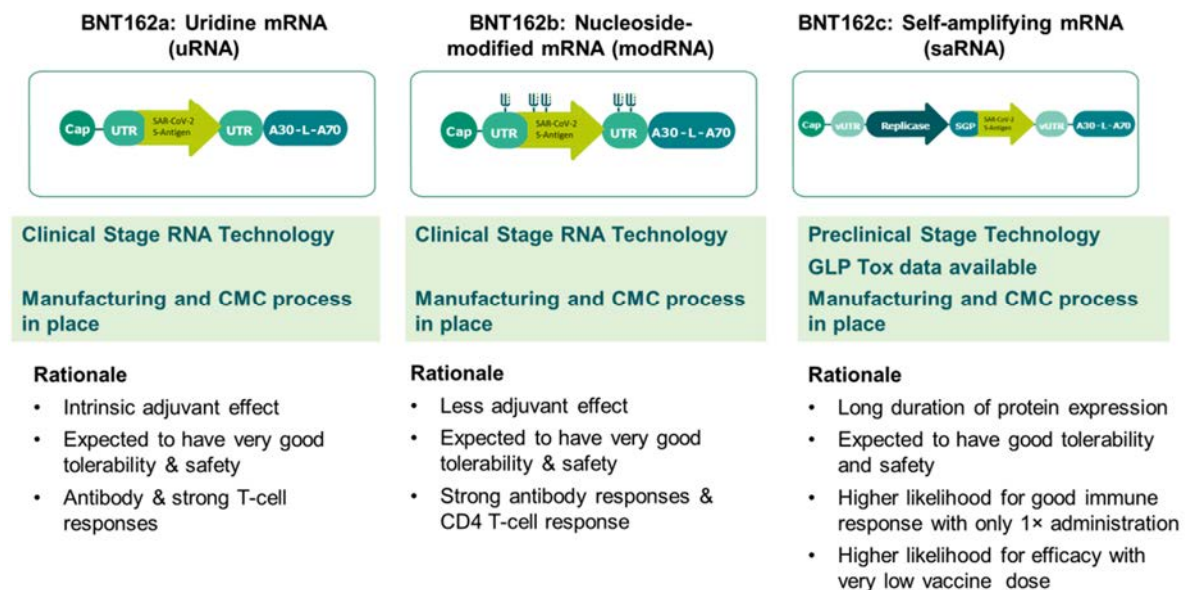
program to develop a prophylactic vaccine to prevent infection with SARS-CoV-2 and its associated disease COVID-19.

#### 2.4.2.1.2. RNA Vaccine Platforms

BioNTech has longstanding and diversified expertise in utilizing messenger RNA (mRNA) to deliver genetic information to cells, where it is used to express proteins for a therapeutic effect. BioNTech has been working in the RNA field for more than a decade with emphasis in the oncology field. Biontech and Pfizer are developing a portfolio of RNA therapies that utilize different mRNA platforms to develop an optimized formulation for a given infectious disease indication with emphasis on preventing viral diseases such as COVID-19.

Biontech is evaluating three RNA platforms in human clinical trials for oncology indications, primarily as repeatedly IV administered therapeutic cancer vaccines, and over 613 patients have been dosed to date. This clinical experience includes many patients who have had long term exposure, i.e., who have received more than 8 IV administrations.

**Figure 2.4.2-1. Overview of the Three RNA Platforms**



The mRNA vaccine molecules are capped and contain ORFs, which are flanked by the UTRs, and polyA-tails at the 3' end. The ORF of the uRNA and modRNA vectors encode the vaccine antigen of interest. Self-amplifying RNA has two ORFs. The first ORF encodes an alphavirus-derived replicase which, upon translation, mediates self-amplification of the RNA. The second ORF encodes the vaccine antigen.

RNA is attractive as a vaccine platform as it enables timely and effective response to emerging infectious disease threats. RNA vaccines can mimic antigen expression during natural infection by directing expression of virtually any pathogen antigen with high precision and flexibility of antigen design. RNA occurs naturally in the body, is metabolized and eliminated by the body's natural mechanisms, does not integrate into the genome, is transiently expressed, and, therefore, is considered safe. Vaccination with RNA in general



generates robust immune responses as RNA not only delivers the vaccine antigen, but also has intrinsic adjuvant effects.

RNA vaccine platform approaches greatly simplify development and manufacturing, irrespective of the encoded pathogen antigens. Thus, RNA has the potential of rapid, cost-efficient, high-volume manufacturing and flexible stockpiling (long term storage of low-volume libraries of frozen plasmid and unformulated RNA, which can be rapidly formulated and distributed). BioNTech has expertise in production process development for various RNA chemistries and formulations. A LNP-formulated RNA-based vaccine would provide one of the most flexible, scalable, and fastest approaches to protect against new, fast spreading, virus infections (Rauch et al, 2018; Sahin et al, 2014).

RNA vaccines are molecularly defined, highly purified immunogens. Unlike live attenuated vaccines, RNA vaccines do not carry the risks associated with infection. RNA-based vaccines are manufactured using a cell-free in vitro transcription process, which allows an easy and rapid production and the prospect of producing high numbers of vaccine doses within a shorter time period than possible with conventional vaccine approaches. This capability is pivotal to enable the most effective response in outbreak scenarios.

In the COVID-19 vaccine candidates, RNA drug substances are formulated with lipids as RNA-LNP drug products. The vaccine candidates are supplied as buffered-liquid solutions for IM injection. The RNA drug substances are highly purified single-stranded, 5'-capped messenger mRNAs produced by in vitro transcription from the corresponding DNA templates, each encoding full-length or parts of the SARS-CoV-2 S glycoprotein.

The RNA components of the COVID-19 vaccine candidates are based on three platforms (Figure 2.4.2-1): unmodified mRNA (uRNA), nucleoside-modified mRNA (modRNA), and self-amplifying RNA (saRNA).

#### **2.4.2.1.2.1. uRNA**

uRNA is single-stranded, 5'-capped mRNA that is translated upon entering the cell. In addition to the open reading frame (ORF) encoding the SARS-CoV-2 antigen, each uRNA contains common structural elements optimized for increased stability and translational efficiency – a 5' cap, 5' untranslated region (UTR), 3' UTR, and poly(A)-tail.

#### **2.4.2.1.2.1. modRNA**

ModRNA is also a single-stranded, 5'-capped mRNA that is translated upon entering the cell. In addition to the ORF encoding the SARS-CoV-2 antigen, each modRNA contains common structural elements optimized for high efficacy of the RNA. Compared to the uRNA, modRNA contains a different 5' cap structure and a substitution of 1-methyl-pseudouridine for uridine. This substitution decreases recognition of the vaccine RNA by innate immune sensors, such as toll-like receptors (TLRs) 7 and 8, resulting in decreased innate immune activation and increased protein translation.

#### **2.4.2.1.2.2. saRNA**

SaRNA is a single-stranded 5'-capped RNA that self-amplifies upon entering the cell. The SARS-CoV-2 antigen is translated as the RNA self-amplifies. A 5' ORF encodes the Venezuelan equine encephalitis (VEE) virus RNA-dependent RNA polymerase (RDRP or replicase). A 3' ORF encodes the SARS-CoV-2 antigen, under control of a subgenomic promoter. The saRNA vector contains additional conserved sequence elements supporting replication and translation, including 5' and 3' UTRs and a poly A tail, but no other VEE virus coding sequences. When saRNA is introduced to the cytoplasm of a cell, ribosomes translate the replicase. The replicase, which also has a capping function, carries out negative strand RNA synthesis and then uses the negative strand copies of the positive strand vaccine RNA to synthesize new complete positive strand RNAs (for replication) and large quantities of the much shorter subgenomic mRNA, which encodes the antigen. The resulting "launch" of saRNA results in high level, intracellular expression of the antigen and innate immune activation to potentiate an adaptive immune response to the expressed antigen.

#### **2.4.2.1.2.3. Summary**

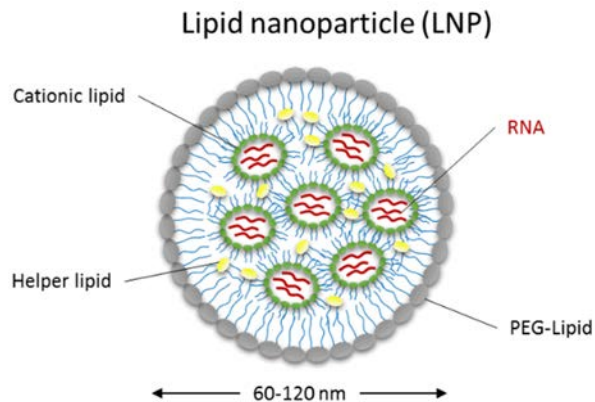
The three RNA platforms have complementary strengths: uRNA, with high intrinsic adjuvanticity; modRNA, with blunted innate immune sensor activating capacity and thus augmented expression of the target antigen; and saRNA, from which higher amounts of protein per injected RNA template can be produced.

The structural elements of the vector backbones of COVID-19 vaccine candidates are optimized for prolonged and strong translation of the antigen-encoding RNA component. The different COVID-19 vaccine RNA platforms exhibit distinct antigen expression profiles after IM injection. All RNA-encoded antigens are expressed transiently. For BNT162a1 (uRNA) and BNT162b1 and BNT162b2 (modRNA), the antigen expression peaks shortly after injection; for BNT162c2 (saRNA), the antigen expression peaks later and is more prolonged due to self-amplification. All vaccine candidates may be administered using prime/boost or prime-only administration regimens.

#### **2.4.2.1.3. Lipid Nanoparticles**

RNAs from each of the platforms are formulated with lipids, which protect the RNA from degradation and enable transfection of the RNA into host cells after IM injection. The same LNP formulation ([Figure 2.4.2-2](#)) is used for all of the COVID-19 vaccine candidates.



**Figure 2.4.2-2. Schematic Organization of a LNP**

The LNPs are composed of four lipids in a defined ratio. During mixing of the RNA and the dissolved lipids, the lipids form the nanoparticles encapsulating the RNA. After injection, the LNPs are taken up by the cells, and the RNA is released into the cytosol. In the cytosol, the RNA is translated, and the encoded viral antigen is produced.

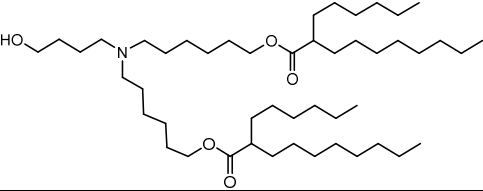
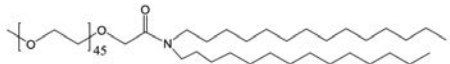
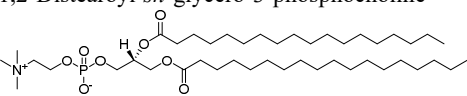
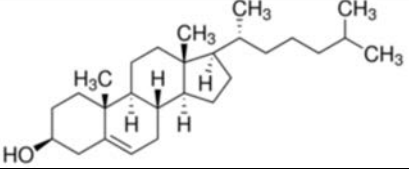
The formulation contains two functional lipids, ALC-0315 and ALC-01592, and, two structural lipids DSPC (1,2-distearoyl-sn-glycero-3-phosphocholine) and cholesterol. The physicochemical properties and the structures of the four lipids are shown in [Table 2.4.2-1](#).

COVID-19 Vaccine (BNT162, PF-07302048)

BB-IND 19736

Module 2.4. Nonclinical Overview

**Table 2.4.2-1. Lipids in the Formulation**

Lipid (CAS number)	Molecular weight [Da]	Molecular formula	Physical state and storage condition	Chemical name (synonyms) and structure
ALC-0315 (not applicable)	766	$C_{48}H_{95}NO_5$	Liquid (oil) -20°C	(4-hydroxybutyl)azanediylbis(hexane-6,1-diyl)bis(2-hexyldecanoate) 
ALC-0159 (1849616-42-7)	~2400-2600	$C_{30}H_{60}NO(C_2H_4O)_nOCH_3$ n=45-50	Solid -20°C	2-[(polyethylene glycol)-2000]-N,N-ditetradecylacetamide 
DSPC (816-94-4)	790	$C_{44}H_{88}NO_8P$	Solid -20°C	1,2-Distearoyl- <i>sn</i> -glycero-3-phosphocholine 
Cholesterol (57-88-5)	387	$C_{27}H_{46}O$	Solid -20°C	

CAS = Chemical Abstracts Service; DSPC = 1,2-distearoyl-*sn*-glycero-3-phosphocholine.

#### 2.4.2.1.4. Immune Phenotype Elicited by LNP-Formulated RNA Vaccines

Due to RNA's inherent adjuvant activity mediated by binding to innate immune sensors such as toll like receptors, RNA-LNP vaccines induce a robust neutralizing antibody response and a concomitant T-cell response resulting in protective immunization with minimal vaccine doses.

The utility of each of the RNA platforms used for development of the COVID-19 vaccine candidates is supported by various nonclinical studies that demonstrate the efficient induction of potent neutralizing antibody and T-cell responses against a variety of viral pathogens including influenza virus, Ebola virus, human immunodeficiency virus (HIV), and Zika virus (Vogel et al, 2018; Moyo et al, 2019; Pardi et al, 2017; Pardi et al, 2018). Unpublished immunogenicity data from RNA based vaccines against other viruses such as Marburg and Lassa virus indicate that the range of applications for anti-viral RNA vaccines is broad (data on file). Moreover, all the mRNA platforms confer strong prophylactic vaccine activity in murine influenza challenge models.

**Table 2.4.2-2. Characteristics of the Adaptive Immune Response for the mRNA Platforms**

	uRNA <sup>a</sup>	modRNA <sup>b</sup>	saRNA <sup>c</sup>
<b>CD4<sup>+</sup> T cell response</b>	<ul style="list-style-type: none"> <li>Induction of multifunctional strongly Th1<sup>+</sup>, skewed immune response with induction of IFN-<math>\gamma</math><sup>+</sup>, TNF-<math>\alpha</math><sup>+</sup>, IL-2<sup>+</sup> CD4<sup>+</sup> T cells.</li> <li>Strong expansion of follicular helper Tfh cells with an IFN-<math>\gamma</math><sup>+</sup>, Tfh cells (mouse, human NHP).</li> </ul>	<ul style="list-style-type: none"> <li>Strong induction of multi-functional Th1 skewed immune response with induction of Th1<sup>+</sup>, IFN-<math>\gamma</math><sup>+</sup>, TNF-<math>\alpha</math><sup>+</sup>, IL-2<sup>+</sup> CD4<sup>+</sup> T cells.</li> <li>Strong expansion of follicular helper Tfh cells with an IFN-<math>\gamma</math><sup>+</sup>, Tfh cells (mouse, human NHP).</li> </ul>	<ul style="list-style-type: none"> <li>Expansion of a strongly Th1 skewed immune response with, multifunctional Th1<sup>+</sup>, IFN-<math>\gamma</math><sup>+</sup>, TNF-<math>\alpha</math><sup>+</sup>, IL-2<sup>+</sup> CD4<sup>+</sup> T cells (mouse).</li> </ul>
<b>CD8<sup>+</sup> T cell response</b>	<ul style="list-style-type: none"> <li>Expansion of multifunctional CD8 cytotoxic, effector and long lived memory T cells with an IFN-<math>\gamma</math><sup>+</sup>, TNF-<math>\alpha</math><sup>+</sup>, CD107<sup>+</sup> phenotype (mouse, human).</li> </ul>	<ul style="list-style-type: none"> <li>Expansion of multifunctional cytotoxic, effector and long lived memory CD8 T cells with an IFN-<math>\gamma</math><sup>+</sup>, TNF-<math>\alpha</math><sup>+</sup>, CD107<sup>+</sup> phenotype (mouse, human).</li> </ul>	<ul style="list-style-type: none"> <li>Strong expansion of long-lived effector and central memory CD8<sup>+</sup> T cells with an IFN-<math>\gamma</math><sup>+</sup>, TNF-<math>\alpha</math><sup>+</sup>, CD107<sup>+</sup> phenotype (mouse).</li> </ul>
<b>Antibody response</b>	<ul style="list-style-type: none"> <li>High-titer, high-affinity, long lived neutralizing antibody responses after prime only/boost (mouse, rats, NHP)</li> <li>ADCC activity (rabbits).</li> <li>Mouse IgG1 ~ IgG2a.</li> </ul>	<ul style="list-style-type: none"> <li>High-titer, high-affinity, long lived neutralizing antibody responses after prime/boost only (mouse, rats, NHP).</li> <li>ADCC activity (rabbits)</li> <li>Mouse IgG1 ~ IgG2a.</li> </ul>	<ul style="list-style-type: none"> <li>High-titer, neutralizing antibody responses after prime only (mouse, rats, pig, NHP).</li> <li>Mouse IgG2a &gt;&gt; IgG1.</li> </ul>

ADCC = Antibody-dependent cellular cytotoxicity; IgG = Immunoglobulin G; IL = interleukin; IFN = Interferon; NHP = Non-human primate; Tfh = T follicular helper; TNF = Tumor necrosis factor; CD = cluster of differentiation.

a. Source: Pardi et al, 2017, 2018, 2019; Vogel et al, 2018, Kranz et al, 2016

b. Source: Vogel et al, 2018, Kranz et al, 2016, Pardi et al, 2017, 2018, 2019

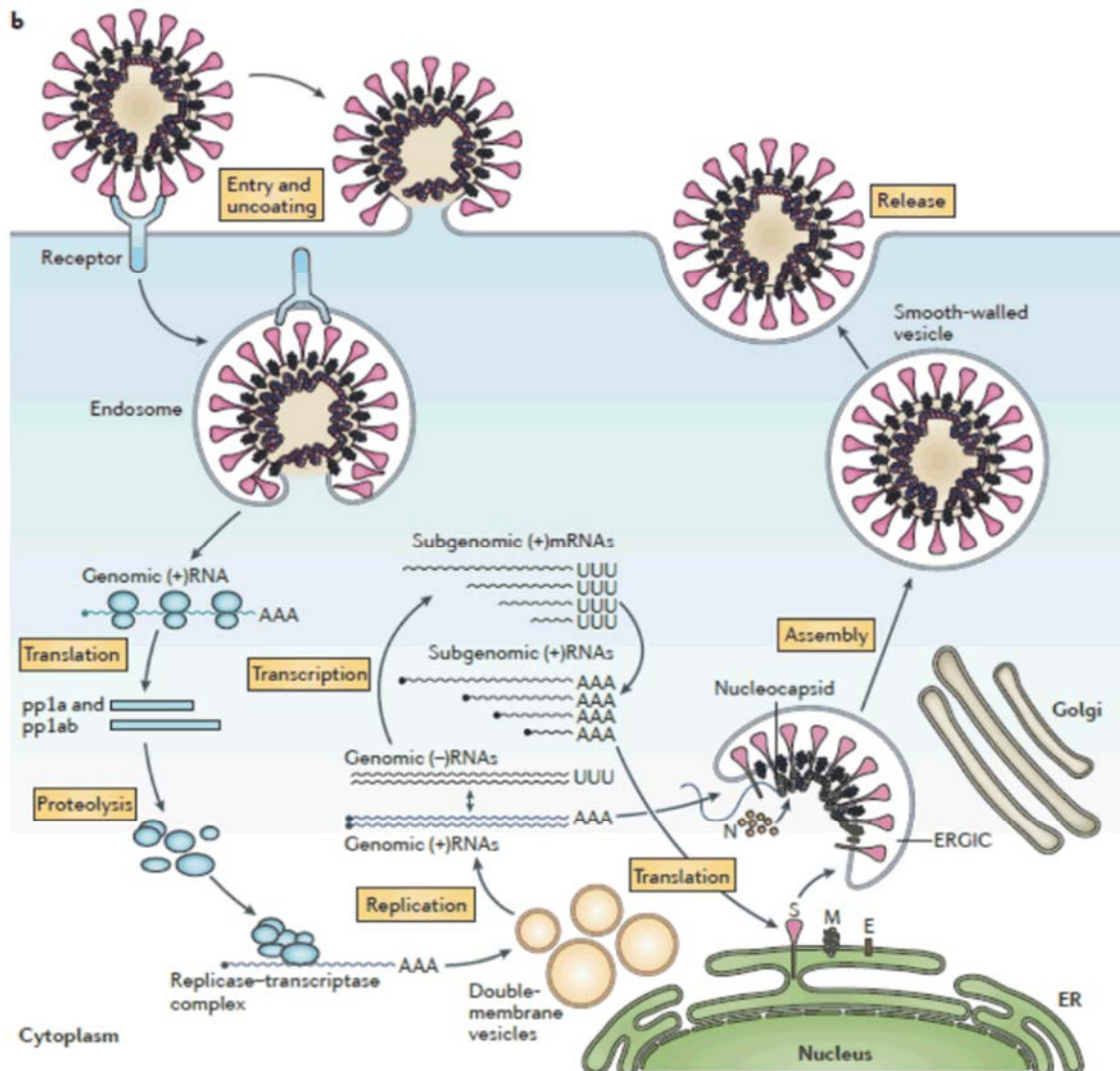
c. Source: Vogel et al, 2018, Moyo et al, 2019

Vaccine candidates based on these mRNA platforms induce strong antibody responses and prime and expand multifunctional CD4 and CD8 positive T cells. The properties of antigen-specific immune responses induced by vaccination with these mRNA formats were studied in several species ([Table 2.4.2-2](#)). Vaccination with modRNA is characterized by the strong expansion of Th1-skewed antigen-specific T follicular helper (Tfh) cells, which stimulate and expand germinal center B cells, thereby resulting in particularly strong, long-lived, high-affinity antibody responses. The uRNA and saRNA formats exhibit a higher immune-stimulatory activity due to their TLR7/8 stimulatory capacity, thereby giving rise to a type-I interferon release, a strongly Th1 biased CD4+ T cell response as well as strong expansion of cytotoxic T cells ([Sahin et al, 2014](#)). Due to self-amplification and prolonged translation saRNA is able to induce strong CD4+ and CD8+ T cell responses by a prime only administration schedule ([Vogel et al, 2018](#)).

#### **2.4.2.1.5. SARS-CoV-2 S as a Vaccine Target**

Coronaviruses, like SARS-CoV-2, are members of a family of enveloped, positive sense, single-stranded RNA viruses ([Figure 2.4.2-3](#)). Coronaviruses encode four structural proteins. Of these, the spike glycoprotein (S) is the key target for vaccine development ([Figure 2.4.2-4](#)). Like influenza virus hemagglutinin (HA), coronavirus S is responsible for receptor-recognition, attachment to the cell, viral envelope fusion with a host cell membrane, and genomic release driven by the S protein conformation change leading to the fusion of viral and host cell membranes. S is cleaved by host proteases into the S1 and S2 fragments. While S2, which is membrane anchored, is responsible for membrane fusion, the S1 fragment, with its C-terminal receptor-binding domain (RBD), recognizes the host receptor and binds to the target host cell. SARS-CoV and SARS-CoV-2 have similar structural properties and bind to the same host cell receptor, angiotensin converting enzyme 2 (ACE-2) ([Zhou et al, 2020](#)).

**Figure 2.4.2-3. Replication Cycle of a Coronavirus**



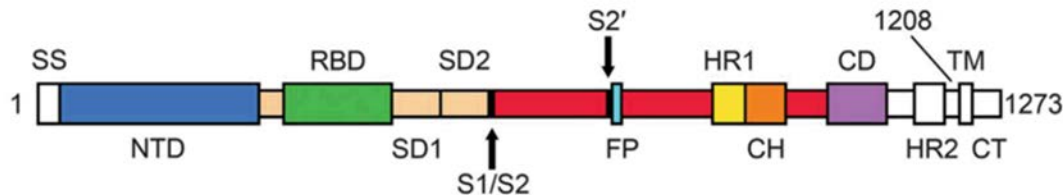
Source: [de Wit et al, 2016](#)

Coronavirus S is pivotal not only for host cell recognition and entry, but also for the induction of virus neutralizing antibodies by the host immune system ([Zakhartchouk et al, 2007](#); [Yong et al, 2019](#)). Some monoclonal antibodies against S, particularly those directed against the RBD, neutralize SARS-CoV and Middle East respiratory syndrome (MERS)-CoV infection in vitro and in vivo ([Hulswit et al, 2016](#)). Targeting the S protein, as well as its S1 cleavage fragment, or the RBD alone, with vaccines is sufficient to induce neutralizing immune responses ([Al-Amri et al, 2017](#)).

The RBD forms membrane distal “heads” on the S protein that are connected to the body by a hinge. In the native S protein, when the RBD is in the “heads down” conformation, the

neutralizing epitopes at the receptor binding site are occluded. When the RBD is in the “heads up” conformation, the neutralizing epitopes at the receptor binding site are exposed. Therefore, a P2 mutant, “heads up” variant of S can elicit a stronger neutralizing antibody response than native S (Pallesen et al, 2017; Wrapp et al, 2020).

**Figure 2.4.2-4. Schematic of the Organization of the SARS-CoV-2 S Glycoprotein**



The S1 fragment includes the signal sequence (SS) and the receptor binding domain (RBD), which is the key subunit within the S protein that is relevant for binding to the human cellular receptor ACE2. The S2 subunit contains the S2 protease cleavage site (S2') followed by a fusion peptide (FP) for membrane fusion, heptad repeats (HR1 and HR2) with a central helix (CH) domain, the transmembrane domain (TM) and a cytoplasmic tail (CT). Source: modified from Wrapp et al, 2020.

The COVID-19 vaccine candidates selected for clinical testing feature the following vaccine antigens (Figure 2.4.2-4).

- A non-membrane anchored receptor binding domain from SARS-CoV-2 S, with a C-terminal T4 fibrin foldon domain added to trimerize the molecule, potentially increasing its immunogenicity (RBD; Kirchdoerfer et al, 2018). One codon optimized form of the coding sequence for this antigen is designated “variant 5” (V5).
- A membrane-anchored full-length S glycoprotein with the mutation of residues in the central helix proline to lock S in an antigenically optimal “heads up” conformation (Wrapp et al, 2020; Pallesen et al, 2017). Two codon optimized forms of the coding sequence for this antigen are designated “variant 8” and “variant 9” (V8 and V9).

The antigen may be incorporated into the cellular membrane or secreted into the extracellular environment and induce an adaptive immune response. In addition, as S protein is the antigen that recognizes and drives infection of the host cells, it is a key target of virus neutralizing antibodies. Furthermore, as RNA-expressed S protein is fragmented intracellularly, the resulting peptides can be presented at the cell surface, triggering a specific T cell-mediated immune response with activity against the virus.

#### 2.4.2.1.6. Serological and Virological Assays

For preclinical immunogenicity studies, a pseudotype neutralization assay (pVNT) has been used as a surrogate of virus neutralization (which, for SARS-CoV-2, requires BSL3 containment). The pVNT is based on a vesicular stomatitis virus (VSV) vector that lacks the



VSV G glycoprotein. The pseudotype virus instead bears the wild type SARS-CoV-2 S glycoprotein, which mediates entry of the pseudovirus into cells. The pseudovirus can be inactivated by the binding of neutralizing antibodies to the S glycoprotein. For both nonhuman primate preclinical studies and the clinical trial, an authentic SARS-CoV-2 neutralization assay rather than the pseudovirus neutralization assay is planned.

For preclinical studies, antigen-based direct immunoassays (ELISA and/or Luminex formats) measure S1-specific (S1 recombinant protein, Sino Biologics) and RBD-specific (recombinant RBD, Sino Biologics) IgG levels in serum samples. For clinical studies and nonhuman primate studies, a direct binding Luminex immunoassay (dLIA) is being developed to quantify S-specific serum antibodies, allowing comparison of SARS-CoV-2 neutralizing antibody titers to S1-binding or RBD-binding IgG levels as a measure of the quality of vaccine responses.

In addition, a SARS-CoV-2 non-vaccine antigen (NVA) assay is being developed to measure antibodies specific for SARS-CoV-2 antigens not present in any of the vaccine candidates being prepared for C4591001. The NVA will permit evaluation of serological responses to SARS-CoV-2 that are the result of natural exposure rather than vaccine-elicited responses.

To detect SARS-CoV-2 virus shedding, a sensitive reverse transcription-polymerase chain reaction (RT-PCR)-based assay will be used to test nasal swab specimens. An FDA-approved molecular diagnostic will be used for screening swabs for SARS-CoV-2 and may be used in further studies. In addition, we are developing a real time quantitative PCR assay that uses the industry's gold standard polymerase to amplify highly conserved regions of the N and E genes. All available genome sequences have been analyzed and suggest that these regions remain stable across the major sequence clades. The assay will be automated, if necessary, to allow for high throughput processing and testing over 100 samples per day.

#### **2.4.2.1.7. Lack of Cell to Cell Spread of saRNA**

The saRNA vector encodes the alphavirus RNA-dependant RNA polymerase and the vaccine antigen but lacks the genes encoding the alphavirus structural proteins required for virus particle formation, genome packaging and propagation from transfected cells to additional cells. Therefore, the saRNA vaccine lacks the capacity to cause a propagating infection. This inherent safety feature of saRNA vaccine design is confirmed by experimental data.

An infectivity assay was performed to test whether saRNA that expresses the Venezuelan equine encephalitis virus (VEE) RNA-dependent RNA polymerase from its 5' ORF and the HA of influenza virus (strain H1N1, A/California/07/2009) from its 3' ORF can spread cell to cell. In this assay, the HA-encoding saRNA was transfected into HEK cells (schematic of the experiment in [Figure 2.4.2-5](#)). After a 24 h incubation, the medium from the transfected cells was transferred onto new acceptor cells, which were then also incubated for 24 h. Surface HA expression on the transfected cells and the acceptor cells was measured by flow cytometry using HA-specific antibody-based staining. As a positive control, A/California/04/2009 influenza virus, which can spread cell to cell and express HA, was used in place of the saRNA in parallel experimental steps. Donor cells expressed HA on the cell

surface when transfected with saRNA encoding HA or infected with influenza virus (Figure 2.4.2-6). HA was not detected on recipient cells incubated with medium from the donor cells transfected with saRNA encoding HA, but HA was detected recipient cells incubated with medium from influenza virus-infected donor cells.

**Figure 2.4.2-5. Design of Assay to Test for saRNA Cell-to-Cell Spread**

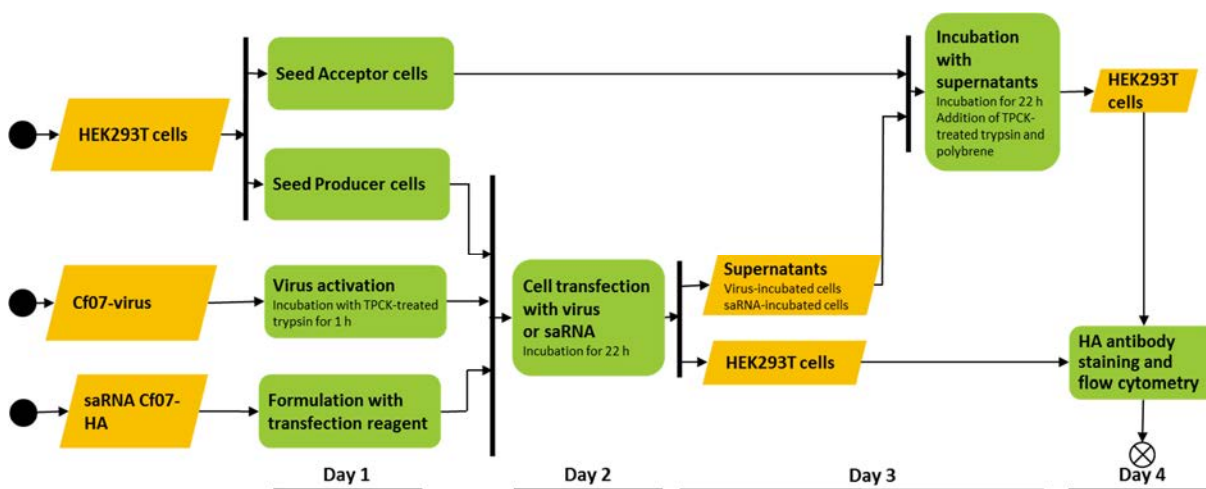
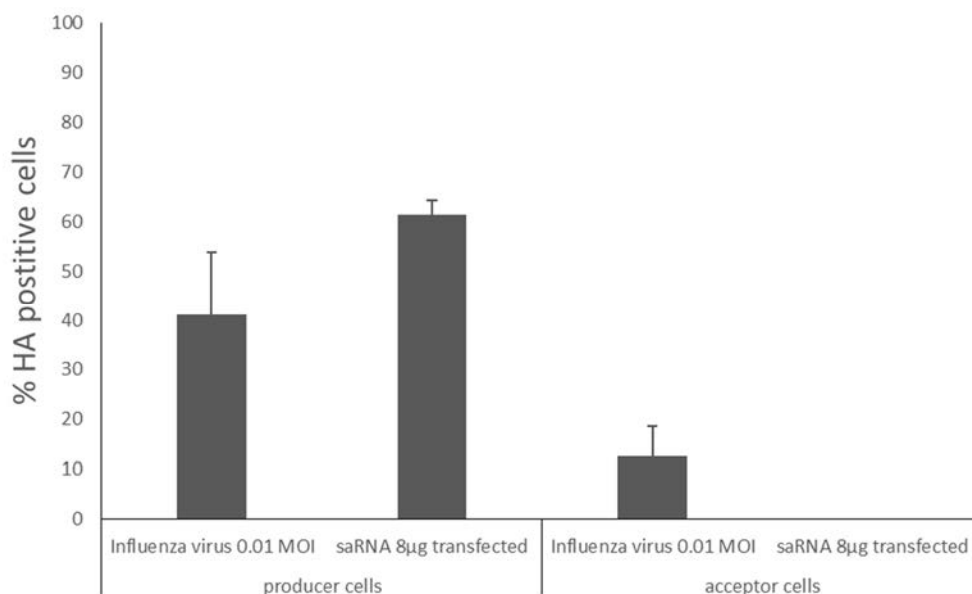


**Figure 2.4.2-6. Flow Cytometry Detection of Cell Surface HA**



Donor cells were analyzed for the presence of HA on the cell surface 24 h after infection or transfection (left). Acceptor cells were analyzed for the presence of HA on the cell surface 24 h after transfer of medium from the donor cells (right). Data give the mean ± SD of triplicate wells for the virus and quadruplicate wells for the saRNA.

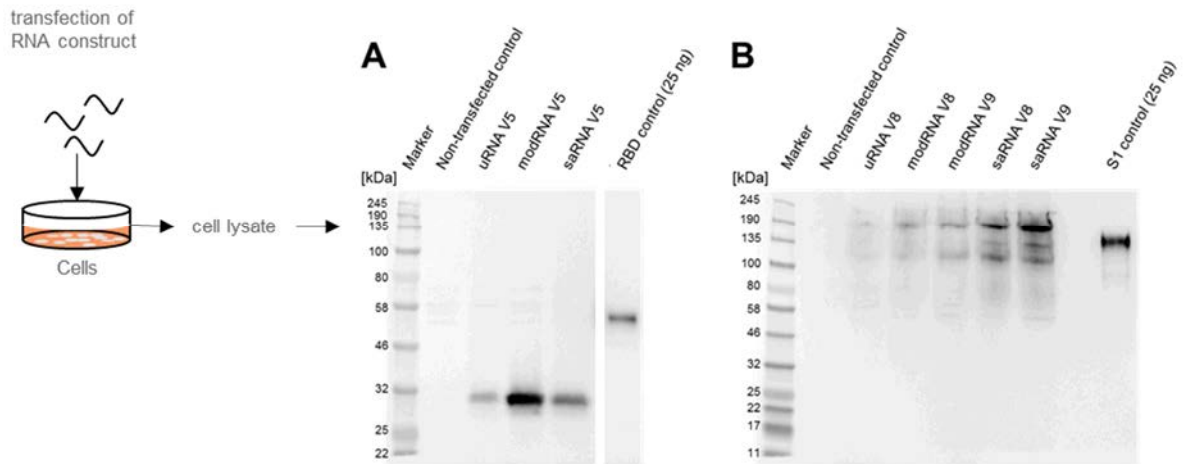


This experiment demonstrates that saRNA encoding HA does not spread cell-to-cell under conditions in which infectious influenza virus does spread cell-to-cell. There is no plausible mechanism for a P2 “heads up” mutant SARS-CoV2 S antigen (Kirchdoerfer et al, 2018) or the RBD in the saRNA platform used for the BNT162c vaccine candidates to mediate cell to cell spread. Therefore, the data with HA-encoding saRNA establish that the saRNA platform does not support cell to cell spread.

#### 2.4.2.1.8. In Vitro Expression of Antigens from COVID-19 vaccine RNA

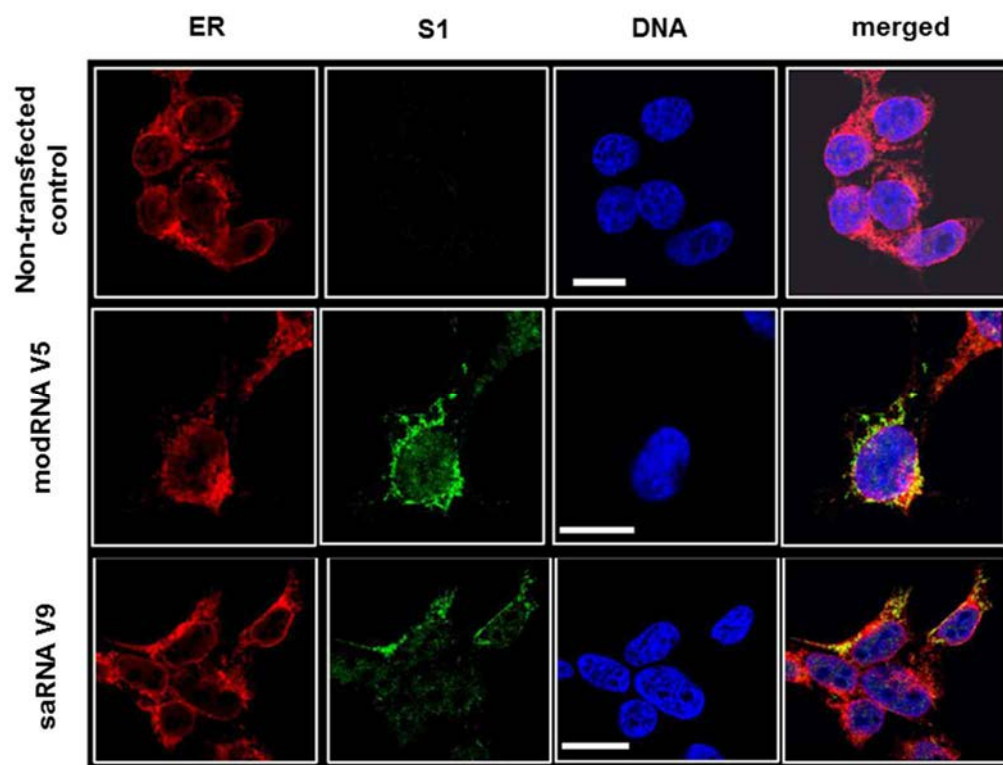
To analyze whether RBD V5, P2 S V8, or P2 S V9 are expressed from the uRNA, modRNA, or saRNA drug substances, HEK 293T cells were transfected with the RNAs, and antigen expression was assessed by western blot (Figure 2.4.2-7), or immunofluorescence microscopy (Figure 2.4.2-8).

**Figure 2.4.2-7. Western Blot Detection of RBD and P2 S in RNA-Transfected Cells**



HEK 293T cells were transfected using RiboJuice™ mRNA transfection reagent (Merck Millipore) with 1 µg of the RNA drug substances (A) uRNA, modRNA, and saRNA encoding RBD V5 and (B) uRNA, modRNA, and saRNA encoding P2 S V8, and modRNA and saRNA encoding P2 S V9. 18 h after transfection, cell lysates were analyzed by a sodium dodecyl sulfate (SDS)–polyacrylamide gel electrophoresis (PAGE) system followed by western blot using a polyclonal antibody that recognizes SARS-CoV-2 S1. All samples showed specific antigen expression, and specific bands were detected for the RBD V5-encoding constructs at the expected apparent MW of 30 kDa and for the P2 S V8 and P2 S V9-encoding constructs at the expected apparent MW of 140 kDa. Recombinant proteins (50 ng RBD, expected apparent MW 52 kDa; 25 ng S1, expected apparent MW 102 kDa) were used as assay controls. RBD V5 was separated with a 10% polyacrylamide gel. P2 S V8 and V9 were separated with a 4–15% polyacrylamide gel.

RBD V5 has a predicted MW of 29.46 kDa, and P2 S V8 and V9 have a predicted MW of 141.14 kDa. Western blot confirmed the presence in lysates of HEK293T cells transfected with the RNA drug substances of proteins that had the expected apparent MWs of the antigens and were recognized by an anti-SARS-CoV-2 S1 polyclonal antibody. This finding confirms expression of the antigens from the RNAs. RBD V5 expression was greatest from the modRNA platform. P2 S expression was greatest from the saRNA platform, with greater expression for the V9 codon optimization variant than for the V8 codon optimization variant.

**Figure 2.4.2-8. Immunofluorescence Detection of RBD and P2 S in RNA Transfected Cells**

HEK293T cells were transfected with 2.5 µg of modRNA encoding RBD V5 or saRNA encoding P2S V9 using RiboJuice™ RNA transfection reagent (Merck Millipore). After 18 h in culture, cells were fixed and stained for the endoplasmic reticulum (ER) with concanavalin A and an Alexa Fluor™ 594 conjugate (red). They were stained for RBD and P2 S with an anti-S1 polyclonal antiserum that recognizes both P2 S and RBD and Alexa Fluor® 488 (green). They were stained for DNA to visualize the nucleus with Hoechst (blue). The merged color panels show that the RBD V5 expressed by modRNA and the P2 S V9 expressed by saRNA each co-localize with the ER marker (scale: 10 µm). A control of non-transfected cells is shown in the top row.

Co-localization of the RBD and P2 S with an endoplasmic reticulum (ER) marker was shown by immunofluorescence microscopy of HEK293T cells transfected with BNT162b1 (modRNA encoding RBD V5) or BNT162c2 (saRNA encoding P2 S V9), respectively (Figure 2.4.2-8).

## 2.4.2.1.9. Supportive Mouse Immunogenicity Studies

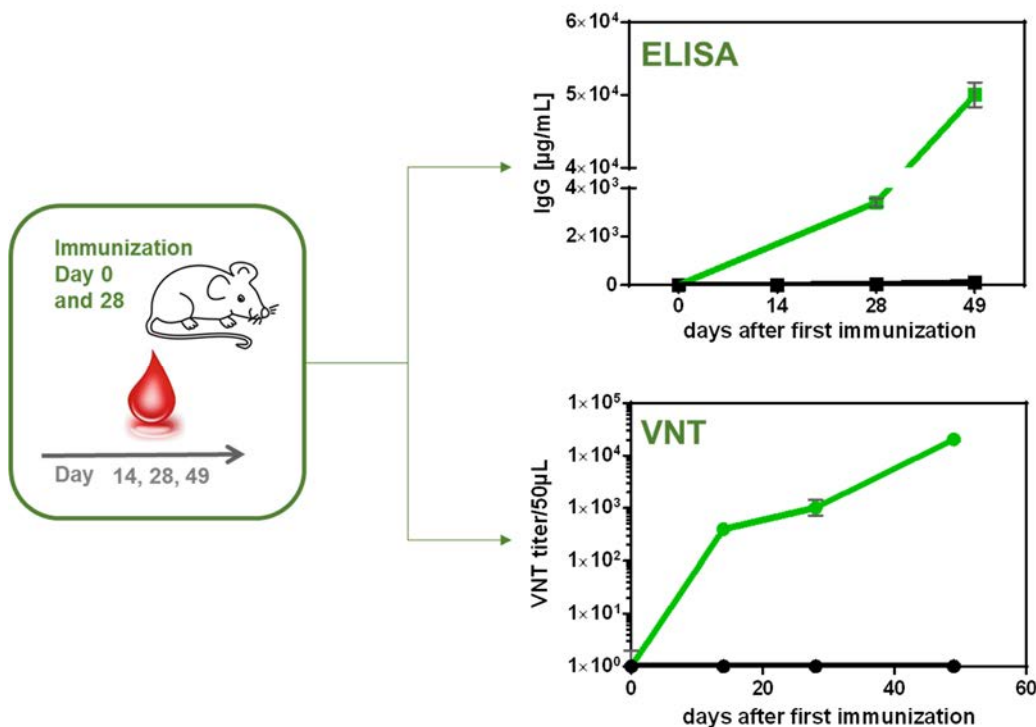
### 2.4.2.1.9.1. Immunogenicity of modRNA Encoding Influenza HA

Because of the extensive knowledge of immunity elicited by influenza HA, including decades of mass influenza immunization and an accepted serological correlate of protection, immunization with LNP-formulated modRNA that encodes influenza HA (H1 A/California/07/2009) provides a benchmark for the platform.

The modRNA was formulated with the same LNP composition that will be used in C4591001. BALB/c mice were immunized IM with 1 µg of the formulated RNA on days 0 and 28. ELISA of sera obtained on days 28 and 49 showed high levels of HA-specific IgG (Figure 2.4.2-9). Sera obtained as early as 14 days after the first dose had high neutralization titers against A/California/07/2009 influenza virus, and by day 49 (21 days after the second dose) serum influenza neutralization titers exceeded  $1 \times 10^4$ .

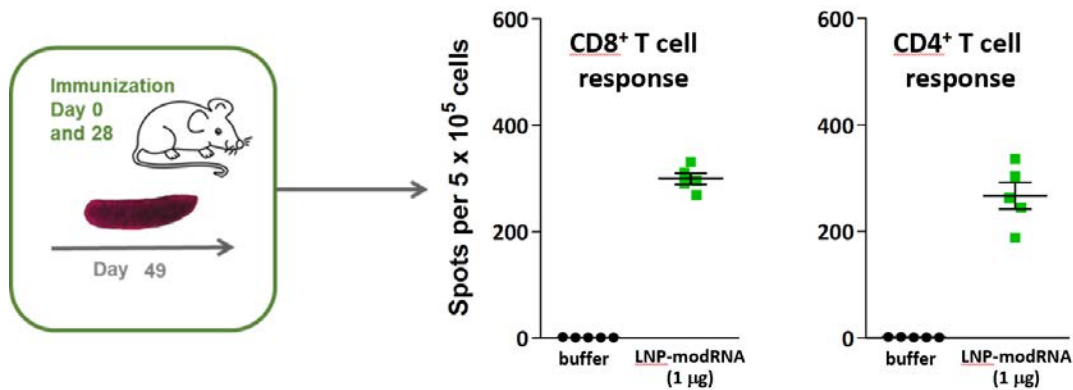
Hemagglutination inhibition (HAI) titers against A/California/07/2009 measured in sera drawn on day 49 were  $1472 \pm 279$  (mean  $\pm$  SEM; data not graphed). This HAI titer greatly exceeds the titer of 40 that is generally accepted as protective against influenza.

**Figure 2.4.2-9. Influenza HA Binding and Virus Neutralization Elicited by Immunization of Mice with modRNA Encoding HA in the Clinical LNP Formulation**



BALB/c mice were immunized twice IM with 1 µg of the vaccine candidate. HA-specific IgG was measured by ELISA. The functionality of the antibodies was measured by influenza virus neutralization.

**Figure 2.4.2-10. CD4<sup>+</sup> and CD8<sup>+</sup> T Cell Response to LNP-Formulated modRNA Encoding Influenza HA by IFN- $\gamma$  ELISpot**



BALB/c mice received two IM immunizations with 1 μg of modRNA encoding influenza HA. The T cell response was analyzed using antigen specific peptides to stimulate T cells recovered from the spleen. Interferon (IFN- $\gamma$ ) release was measured after peptide stimulation using an ELISpot assay.

IFN- $\gamma$  ELISpot on splenocytes harvested on day 49 and stimulated with antigen-specific peptides showed strong CD4<sup>+</sup> and CD8<sup>+</sup> T cell responses (Figure 2.4.2-10). These data confirm that modRNA, formulated with the LNPs that will be used in C4591001 elicit Th1 phenotype T cell responses.

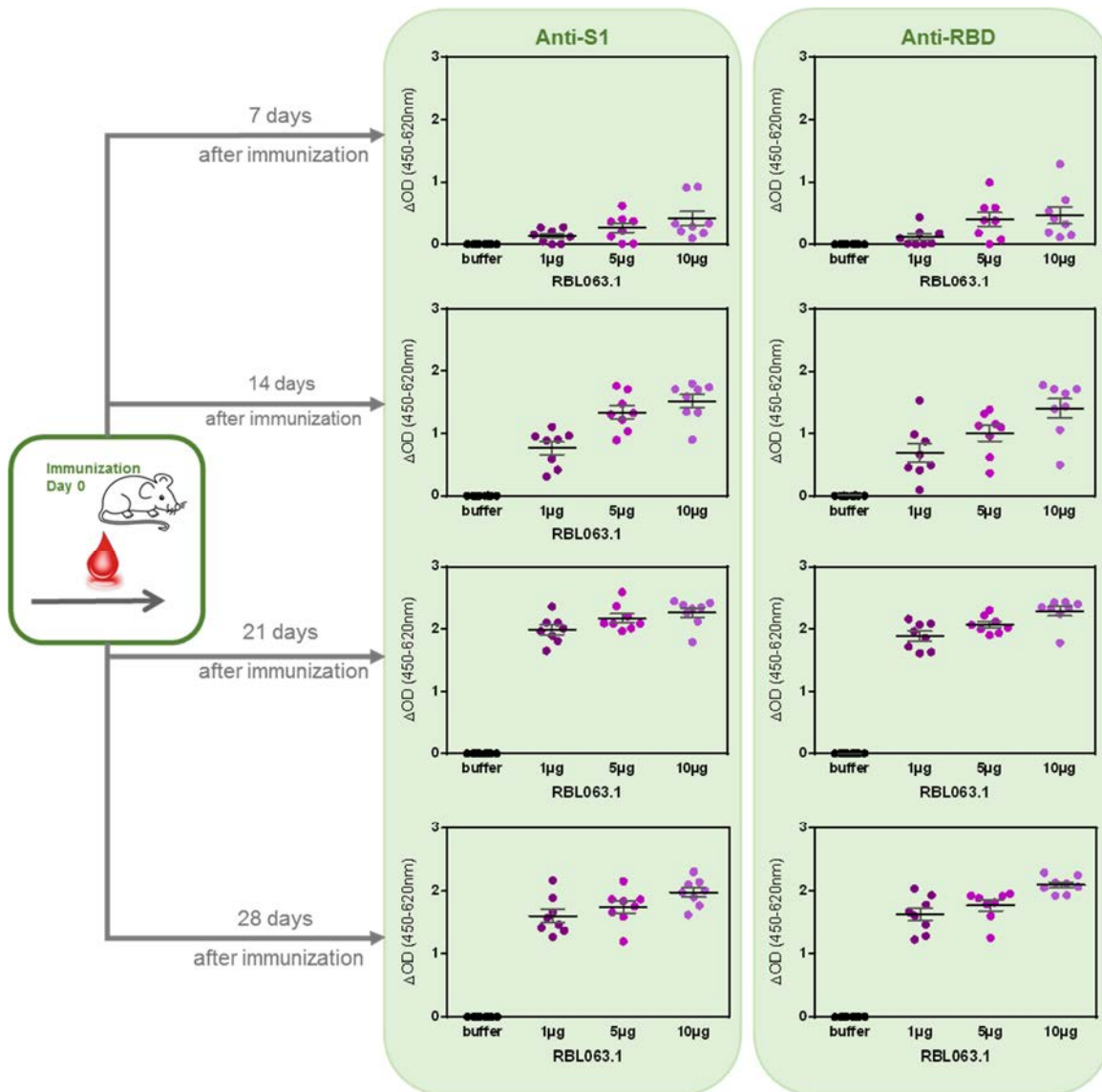
Various other immunogenicity studies in mice have documented the induction of neutralizing antibodies and antigen-specific Th1 type T cell responses with uRNA and saRNA vaccines encoding influenza HA (Vogel et al, 2018). These data were consistent across indications and models and document the immune response profile expected for RNA vaccines.

#### 2.4.2.1.9.2. Immunogenicity of uRNA Encoding P2 S V8 (BNT162a2/RBL063.1)

Note that uRNA encoding RBD, not P2 S, is being prepared for clinical testing.

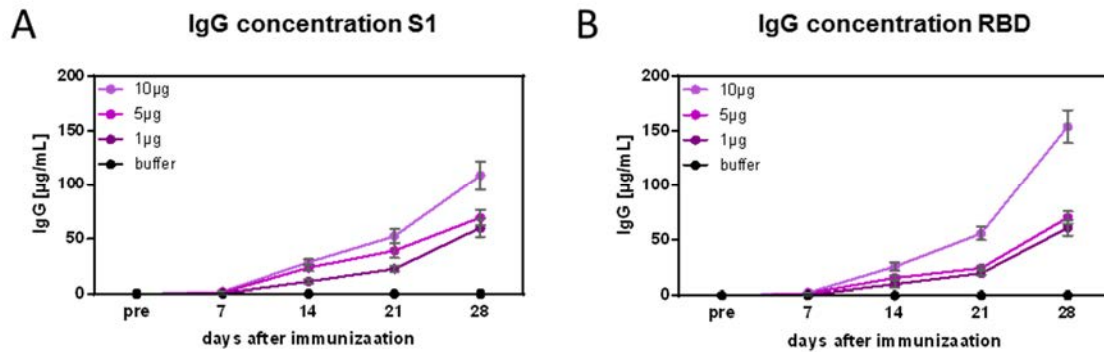
The immunogenicity of LNP-formulated uRNA encoding P2 S V8 was tested in mice (experimental details described in the legends to Figure 2.4.2-11 - Figure 2.4.2-13). ELISA data show an early, dose-dependent IgG response recognizing S1 and the RBD (Figure 2.4.2-11). Concentrations of IgG recognizing S1 (Figure 2.4.2-12A) and RBD (Figure 2.4.2-12B) increased over time. Sera obtained 14, 21 and 28 d after immunization showed dose-dependent SARS-CoV-2 pseudovirus neutralization (Figure 2.4.2-13). The study is ongoing.

**Figure 2.4.2-11. IgG Response Recognizing S1 and RBD 7, 14, 21, and 28 d after Immunization with uRNA Encoding P2 S V8**



BALB/c mice were immunized IM once with 1, 5 or 10  $\mu g$  of LNP-formulated RBL063.1. On 7, 14, 21 and 28 d after immunization, animals were bled, and the serum samples were analyzed for anti-S1 (left) and anti-RBD (right) antigen-specific IgG by ELISA. For day 7 (1:100), day 14 (1:100), day 21 (1:300) and d28 (1:900) results from different serum dilutions are depicted on the graphs. One point in the graph stands for one mouse. Every mouse serum was measured in duplicate. Group size n=8. Mean  $\pm$  SEM are depicted by the horizontal lines with whiskers for each group.

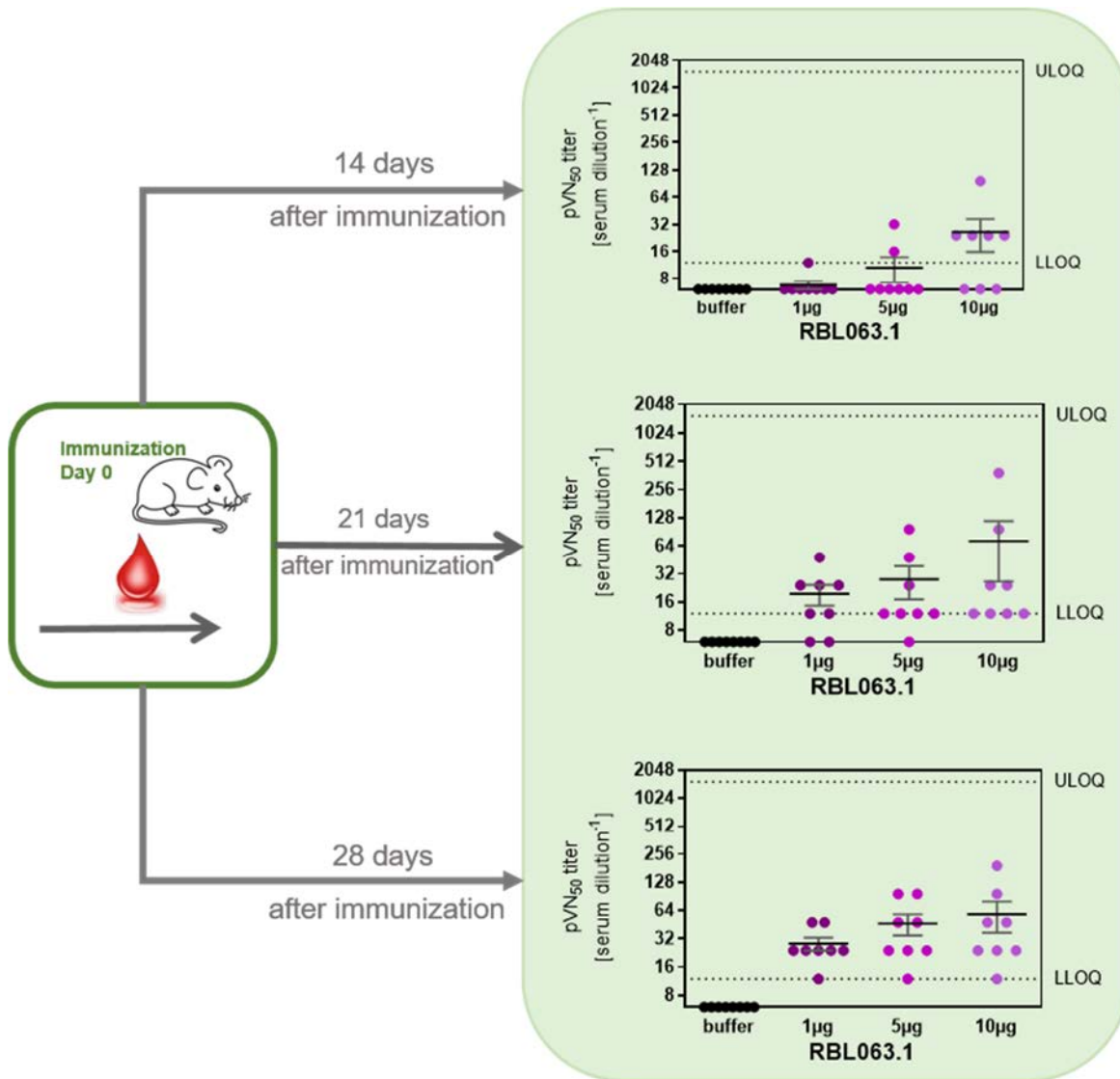
**Figure 2.4.2-12. Kinetics of the IgG Response Recognizing S1 and RBD after Immunization with uRNA Encoding P2 S V8**



For individual  $\Delta$ OD values, the antibody concentrations in the serum samples were calculated. The serum samples were tested against (A) the S1 protein and (B) RBD. Group mean antibody concentrations are shown ( $\pm$ SEM).



**Figure 2.4.2-13. Pseudovirus Neutralization 14, 21 and 28 d after Immunization with uRNA Encoding P2 S V8**

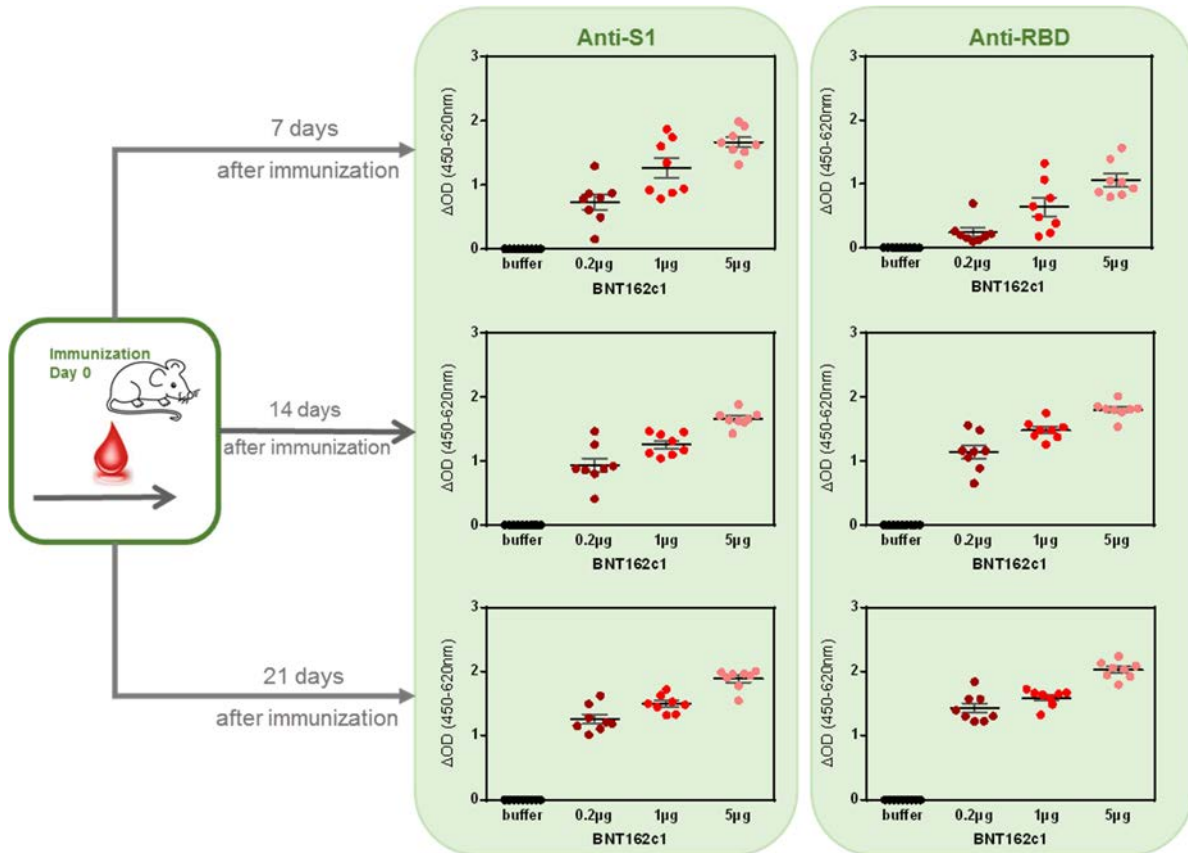


BALB/c mice were immunized IM once with 1, 5 or 10 µg of LNP-formulated RBL063.1. On 14, 21 and 28 d after immunization, animals were bled, and the sera were tested for SARS CoV-2 pseudovirus neutralization. Graphs depict pVN<sub>50</sub> serum dilutions (50% reduction of infectious events, compared to positive controls without serum). One point in the graphs stands for one mouse. Every mouse sample was measured in duplicate. Group size n=8. Mean ± SEM is shown by horizontal bars with whiskers for each group. LLOQ, lower limit of quantification. ULOQ, upper limit of quantification.

#### 2.4.2.1.9.3. Immunogenicity of saRNA Encoding the RBD V5 (BNT162c1/RBL004.3)

The immunogenicity of LNP-formulated saRNA encoding RBD V5 was tested in mice (experimental details in the figure legends). ELISA data show an early, dose-dependent IgG response recognizing S1 and RBD (Figure 2.4.2-14). Pseudotype neutralizing titers are detected 14 d after immunization (Figure 2.4.2-15). The study is ongoing.

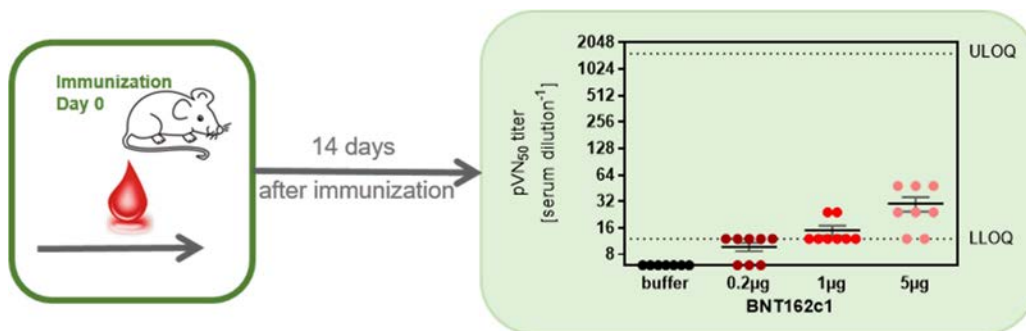
**Figure 2.4.2-14. IgG Response Recognizing S1 and RBD 7, 14 and 21 d after Immunization with saRNA Encoding RBD V5**



BALB/c mice were immunized IM once with 0.2, 1 or 5 μg of LNP-formulated RBS004.3. 7, 14 and 21 d after immunization, animals were bled and the serum samples were analyzed for total amount of anti-S1 (left) and anti-RBD (right) antigen specific immunoglobulin G (IgG) measured via ELISA. For day 7 (1:100), day 14 (1:300) and days 21 (1:900) different serum dilution were included in the graph. One point in the graph stands for one mouse, every mouse sample was measured in duplicates (group size n=8; mean ± SEM is included for the groups).



**Figure 2.4.2-15. Pseudovirus Neutralization 14 d after Immunization with saRNA Encoding the RBD V5**



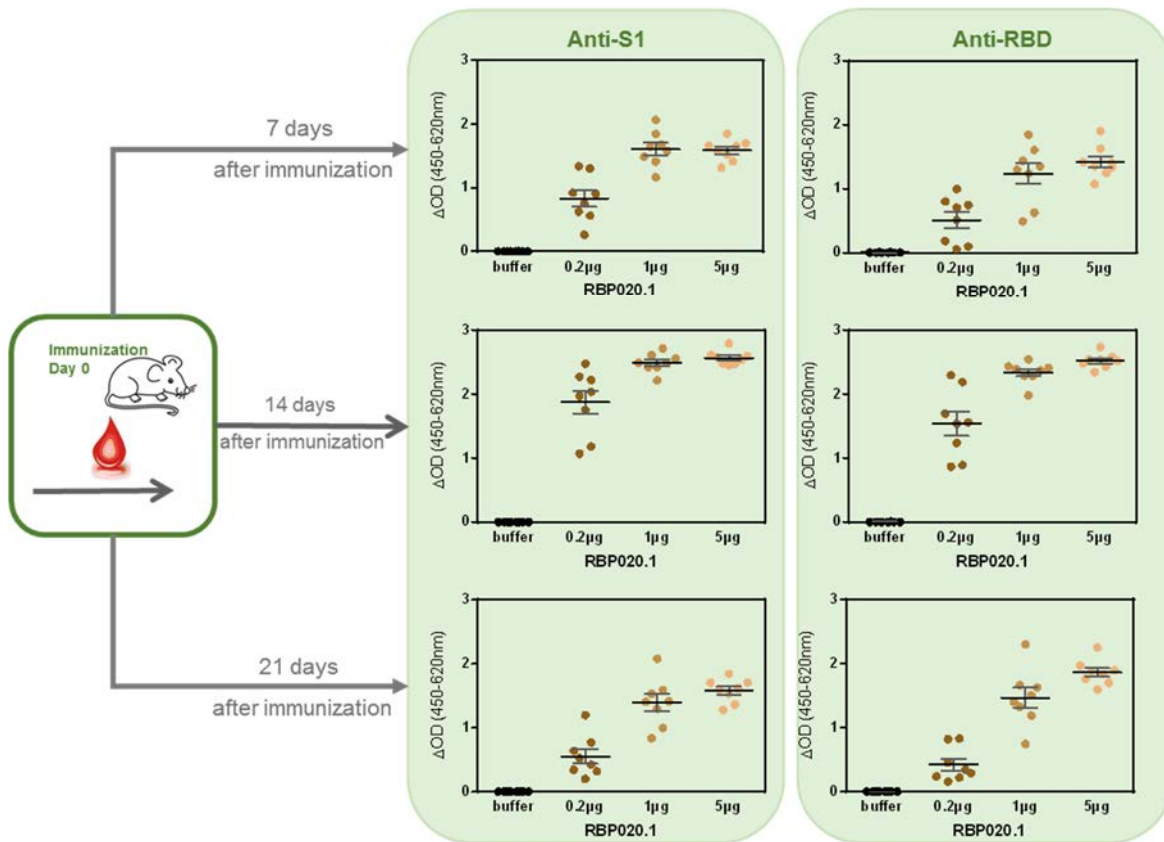
BALB/c mice were immunized IM once with 0.2, 1 or 5 µg of LNP-formulated RBS004.3. On 14 d after immunization, animals were bled and the sera were tested for SARS CoV-2 pseudovirus neutralization. Graphs depict pVN<sub>50</sub> serum dilutions (50% reduction of infectious events, compared to positive controls without serum). One point in the graphs stands for one mouse. Every mouse sample was measured in duplicate. Group size n=8. Mean ± SEM is shown by horizontal bars with whiskers for each group. LLOQ, lower limit of quantification. ULOQ, upper limit of quantification.

#### 2.4.2.1.9.4. Immunogenicity of modRNA Encoding P2 S V8 (BNT162b2/RBP020.1)

Note that modRNA encoding P2 S V9, not P2 S V8, is being prepared for clinical testing.

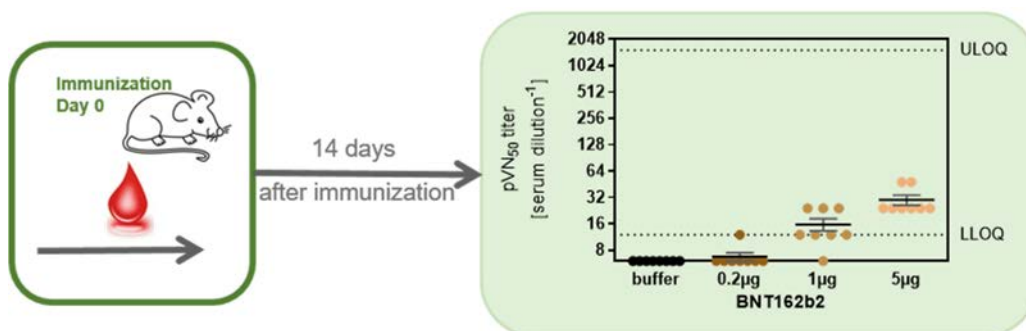
The immunogenicity of LNP-formulated modRNA encoding P2 S V8 was tested in mice (experimental details in the figure legends). ELISA data show an early, dose-dependent IgG response recognizing S1 and RBD (Figure 2.4.2-16). Dose-dependent pseudotype neutralizing titers are detected 14 d after immunization (Figure 2.4.2-17). The study is ongoing.

**Figure 2.4.2-16. IgG Response Recognizing S1 and RBD IgG 7, 14 and 21 d after Immunization with modRNA Encoding P2 S V8**



BALB/c mice were immunized IM once with 0.2, 1 or 5  $\mu g$  of LNP-formulated modRNA RBP020.1. 7, 14 and 21 d after immunization, animals were bled and the serum samples were analyzed for total amount of anti-S1 (left) and anti-RBD (right) antigen specific immunoglobulin G (IgG) measured via ELISA. For day 7 (1:100), day 14 (1:300) and day 21 (1:1100) different serum dilution were included in the graph. One point in the graph stands for one mouse, every mouse sample was measured in duplicates (group size n=8; mean  $\pm$  SEM is included for the groups).

**Figure 2.4.2-17. Pseudovirus Neutralization 14 d after Immunization with modRNA Encoding P2 S V8**



BALB/c mice were immunized IM once with 0.2, 1 or 5 µg of LNP-formulated modRNA RBP020.1. On 14 d after immunization, animals were bled and the sera were tested for SARS CoV-2 pseudovirus neutralization. Graphs depict pVN<sub>50</sub> serum dilutions (50% reduction of infectious events, compared to positive controls without serum). One point in the graphs stands for one mouse. Every mouse sample was measured in duplicate. Group size n=8. Mean ± SEM is shown by horizontal bars with whiskers for each group. LLOQ, lower limit of quantification. ULOQ, upper limit of quantification.

#### 2.4.2.1.10. Mouse Immunogenicity Studies for COVID-19 Vaccine Candidates

Mouse immunogenicity studies are currently ongoing for all COVID-19 vaccine candidates: BNT162a1 (RBL063.3), BNT162b1 (RBP020.3), BNT162b2 (RBP020.2), and BNT162c2 (RBS004.2). Antigen-specific IgG binding levels and pseudovirus neutralizing titers from time points after a single dose of vaccine are available for all candidates and show immunogenicity for both RBD V5 and P2 S V9. Updates will be provided.

**Table 2.4.2-3. Design of Mouse Immunogenicity Studies for COVID-19 Vaccine Candidates**

Group no	No of animals	Vaccine dose	Immunization day	Dose volume [µL] / route	Blood collection day	End of in-life phase
1	8	Buffer	0	20 / IM	7, 14, 21, 28	28
2	8	Low	0	20 / IM	7, 14, 21, 28	28
3	8	Medium	0	20 / IM	7, 14, 21, 28	28
4	8	High	0	20 / IM	7, 14, 21, 28	28

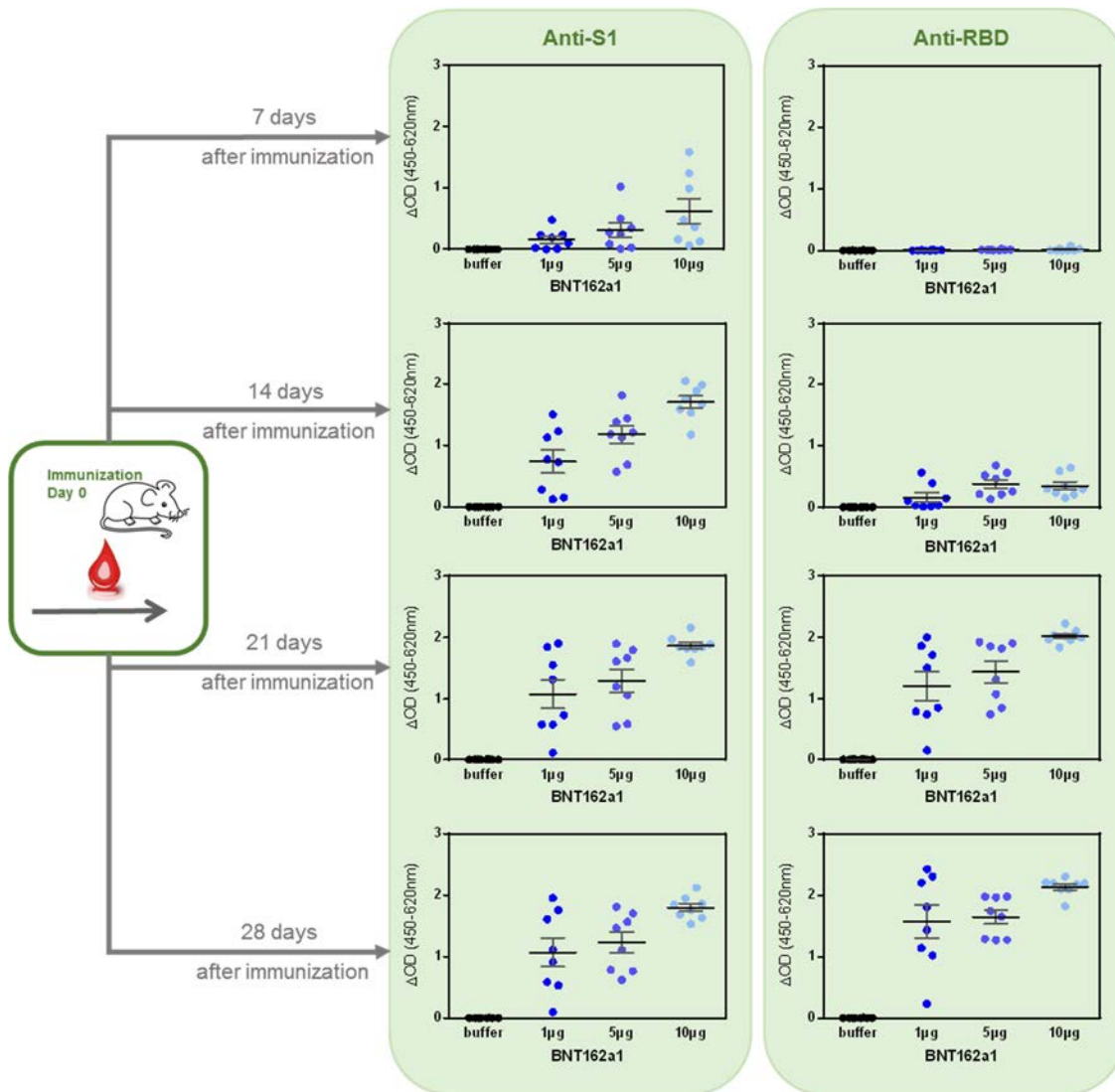
##### 2.4.2.1.10.1. Immunogenicity of uRNA Encoding RBD V5 (BNT162a1/RBL063.3)

The immunogenicity of LNP-formulated uRNA encoding RBD V5 (vaccine candidate BNT162a1) was tested in mice (experimental details in Table 2.4.2-3 and the figure legends). ELISA data show an early, dose-dependent IgG response recognizing S1 and RBD (Figure 2.4.2-18). Antibody concentrations in the serum samples were calculated for the individual sampling days, and the kinetics of IgGs against S1 and RBD proteins are shown in Figure 2.4.2-19. Concentrations of IgG recognizing S1 increased in a dose-dependent manner to d21 and but did not increase further at d28 (Figure 2.4.2-19A). Concentrations of IgG recognizing RBD increased over time in a dose-dependent manner to D28

(Figure 2.4.2-19B). Sera obtained 14, 21 and 28 d after immunization showed minimal to no SARS-CoV-2 pseudovirus neutralization at any dose (Figure 2.4.2-20). The study is ongoing.

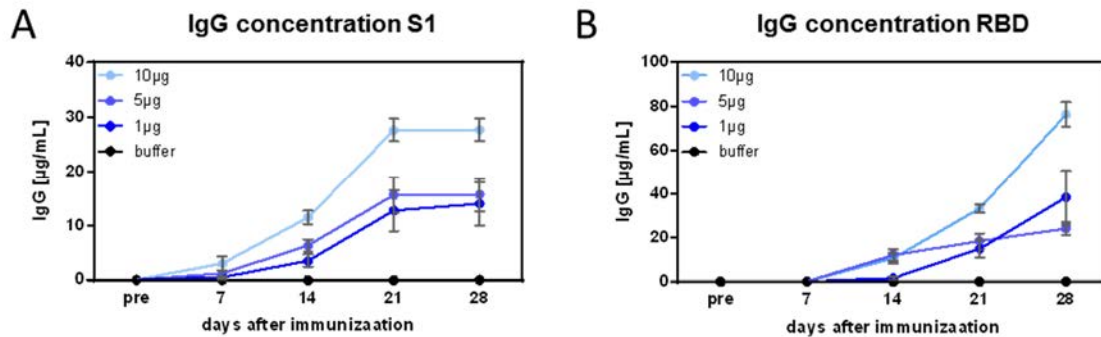
The lack of pseudovirus neutralization activity after a single dose of this vaccine candidate in mice contrasts with the pseudovirus neutralization titers elicited by this candidate after three weekly IM immunizations at the human dose levels in rats (Section 2.4.2.1.11). These findings suggest that the dose levels used in mice for this candidate may have been suboptimal, that more than one dose may be needed to elicit a response, or that the candidate is more immunogenic in rats.

**Figure 2.4.2-18. IgG Response Recognizing S1 and RBD 7, 14, 21 and 28 d after Immunization with uRNA Encoding RBD V5**



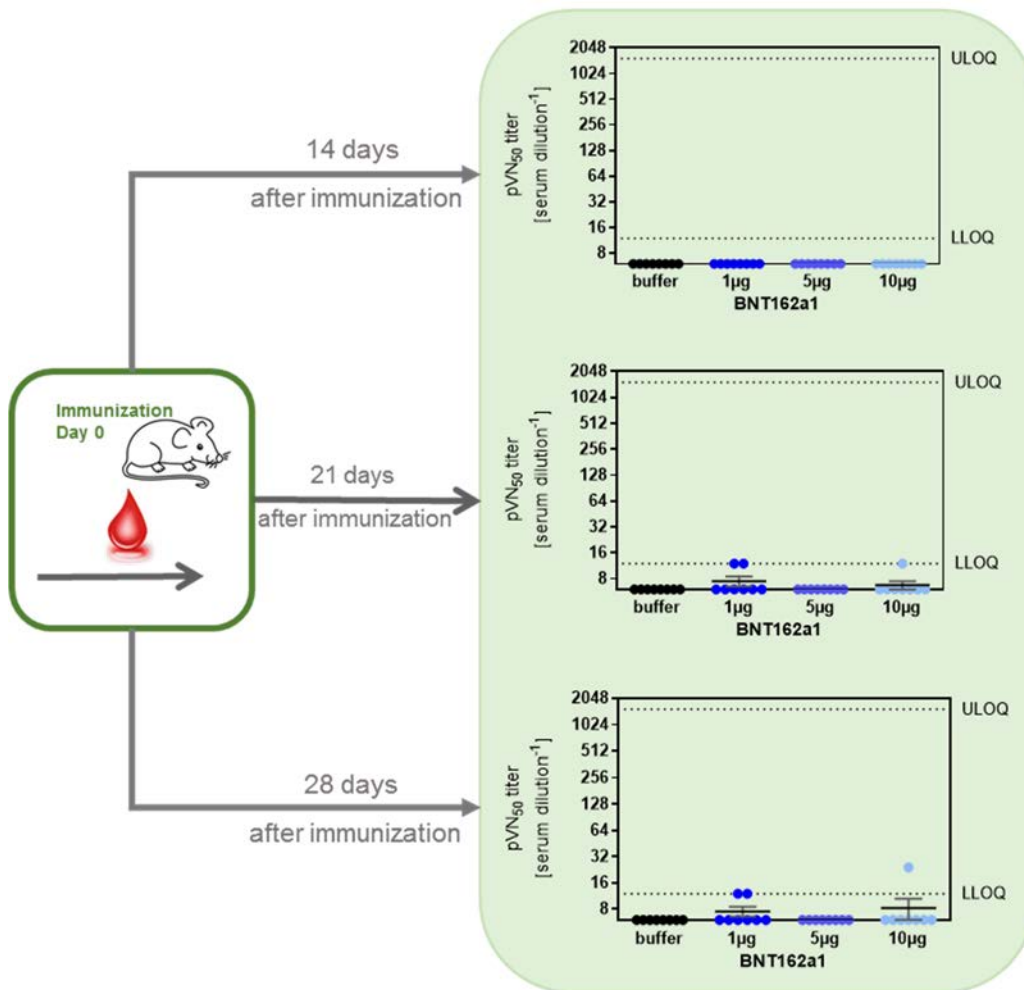
BALB/c mice were immunized IM once with 1, 5 or 10  $\mu g$  of LNP-formulated RBL063.3. On 7, 14, 21 and 28 d after immunization, animals were bled, and the sera were analyzed for anti-S1 (left) and anti-RBD (right) antigen-specific IgG by ELISA. On 7, 14, 21 and 28 d after immunization, animals were bled, and the sera were analyzed for anti-S1 (left) and anti-RBD (right) antigen-specific IgG by ELISA. For all time points, values for a serum dilution of 1:100 were included on the graphs. One point in the graph stands for one mouse. Every mouse sample was measured in duplicate. Group size n=8. Mean  $\pm$  SEM is depicted as a horizontal line with whiskers for each group.

**Figure 2.4.2-19. Kinetics of the IgG Response Recognizing S1 and RBD after Immunization with uRNA Encoding RBD V5**



For individual  $\Delta$ OD values, the antibody concentrations in the serum samples were calculated. The serum samples were tested against (A) the S1 protein and (B) RBD. Group mean antibody concentrations are shown ( $\pm$ SEM). Note that for the S1 and the RBD, 1 mg/mL protein were coated onto a 96 well plate. BNT162b2 encodes the RBD only. As the RBD is smaller than S1, more antibody binding sites are available in 1 mg/mL of RBD compared to S1 which could explain the higher antibody concentration calculated against RBD.

**Figure 2.4.2-20. Pseudovirus Neutralization Titers 7, 14, and 21 after Immunization with uRNA Encoding RBD V5**



BALB/c mice were immunized IM once with 1, 5 or 10 µg of BNT162a1. On 14, 21 and 28 d after immunization, animals were bled, and the sera were tested for SARS CoV-2 pseudovirus neutralization. Graphs depict pVN<sub>50</sub> serum dilutions (50% reduction of infectious events, compared to positive controls without serum). One point in the graphs stands for one mouse. Every mouse sample was measured in duplicate. Group size n=8. Mean ± SEM is shown by horizontal bars with whiskers for each group. LLOQ, lower limit of quantification. ULOQ, upper limit of quantification.

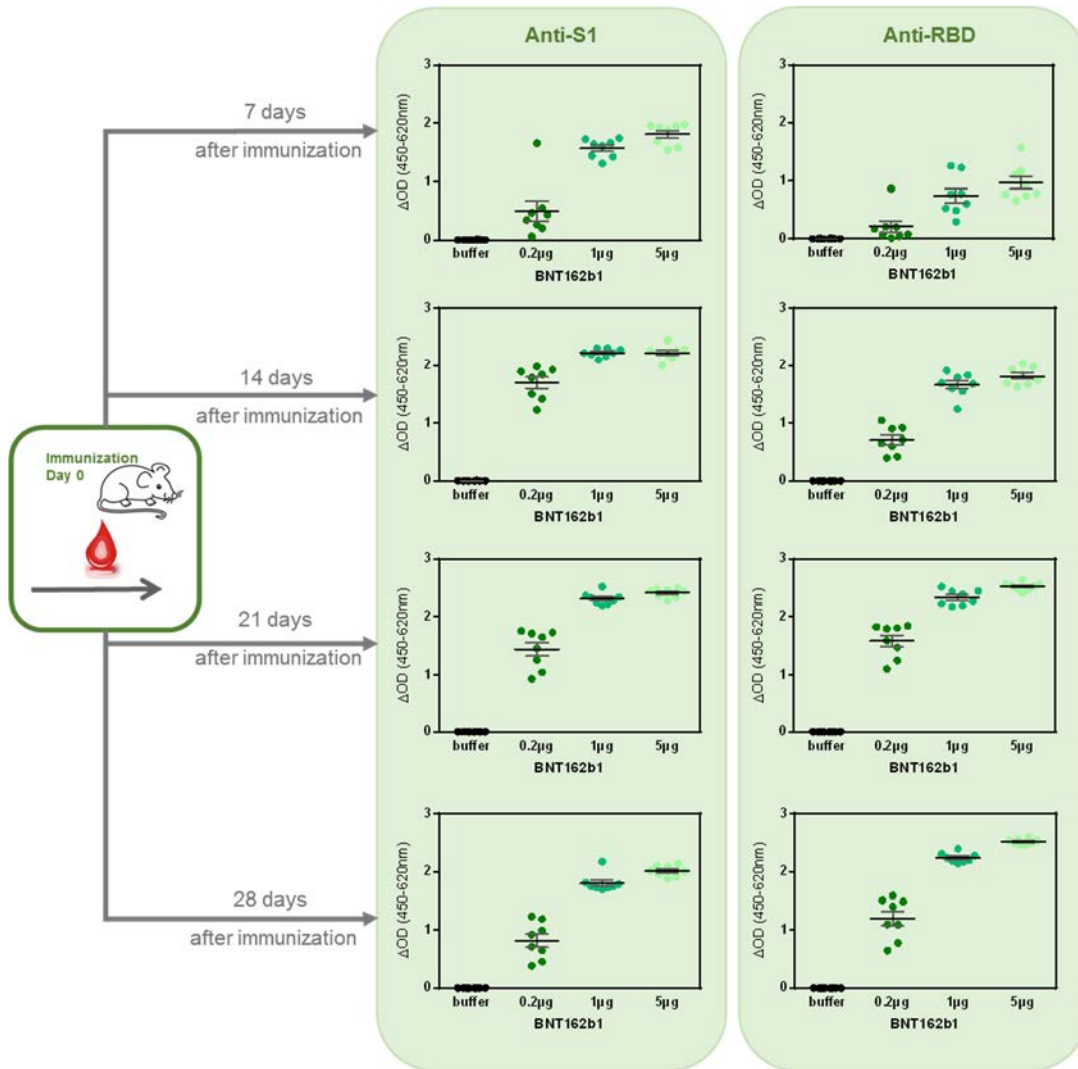
#### 2.4.2.1.10.2. Immunogenicity of modRNA Encoding RBD V5 (BNT162b1/RBP020.3)

The immunogenicity of LNP-formulated modRNA encoding RBD V5 (vaccine candidate BNT162b1) was tested in mice (experimental details in [Table 2.4.2-3](#) and the figure legends). ELISA data show an early, dose-dependent IgG response recognizing S1 and RBD ([Figure 2.4.2-21](#)). Antibody concentrations in the serum samples were calculated for the individual sampling days, and the kinetics of IgGs against S1 and RBD proteins are shown in [Figure 2.4.2-22](#). Antibody concentrations against S1 ([Figure 2.4.2-22A](#)) and RBD ([Figure 2.4.2-22B](#)) increased in a dose-dependent manner over time. Sera obtained 14, 21



and 28 d after immunization show dose-dependent pseudovirus neutralization (Figure 2.4.2-23). The study is ongoing.

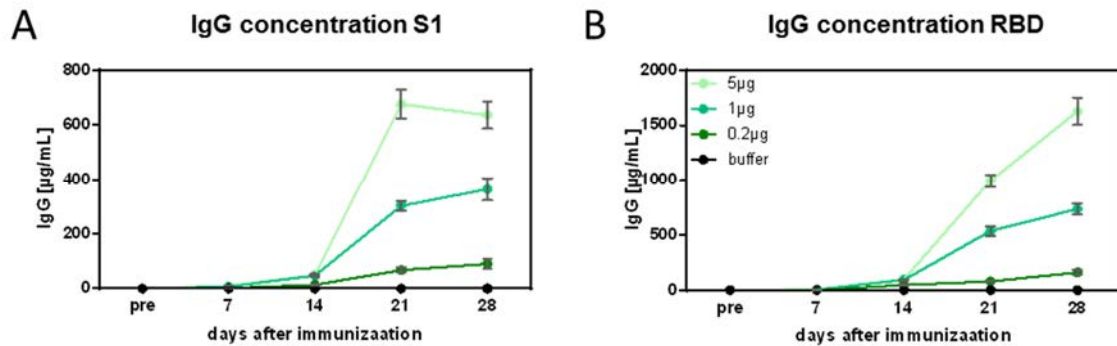
**Figure 2.4.2-21. IgG Response Recognizing S1 and RBD 7, 14, 21 and 28 d after Immunization with modRNA Encoding RBD V5**



BALB/c mice were immunized IM once with 0.2, 1 or 5 µg of LNP-formulated modRNA vaccine candidate encoding the RBD (BNT162b1). On 7, 14, 21 and 28 d after immunization, animals were bled, and the sera were analyzed for anti-S1 (left) and anti-RBD (right) antigen-specific IgG by ELISA. For day 7 (1:100), day 14 (1:300), day 21 (1:900) and day 28 (1:2700), data from different serum dilutions were included on the graphs. One point on the graphs stands for one mouse. Every serum sample was measured in duplicate. Group size n=8. Mean  $\pm$  SEM is depicted by a horizontal line with whiskers for each group.

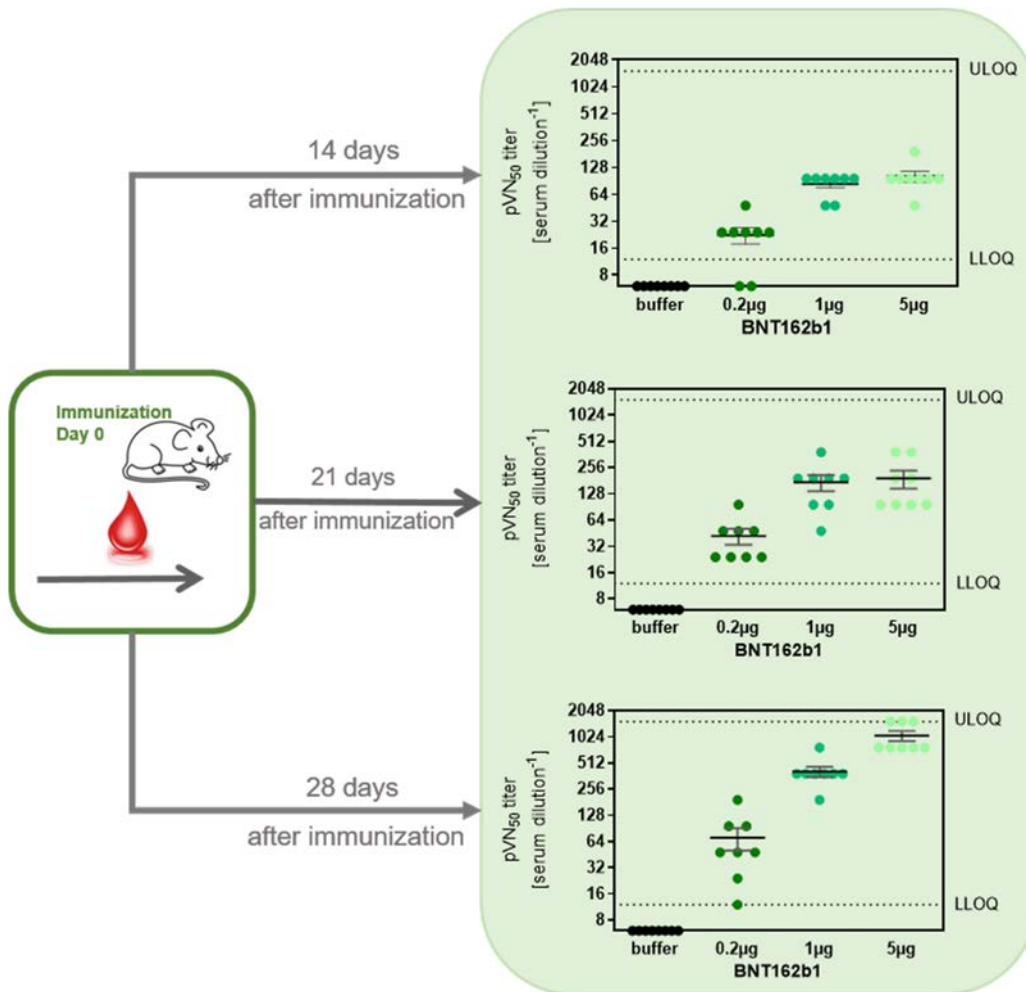


**Figure 2.4.2-22. Kinetics of the IgG Response Recognizing S1 and RBD after Immunization with modRNA Encoding RBD V5**



For individual  $\Delta$ OD values, the antibody concentrations in the serum samples were calculated. The serum samples were tested against (A) the S1 protein and (B) RBD. Group mean antibody concentrations are shown ( $\pm$ SEM). Note that for the S1 and the RBD, 1mg/mL protein were coated onto a 96well plate. BNT162b2 encodes for the receptor binding domain only. As the RBD has a smaller size than the S1, more antibody binding sites are available within 1 mg/mL of RBD compared to S1 which could explain the higher antibody concentration calculated against RBD.

**Figure 2.4.2-23. Pseudovirus Neutralization 14, 21 and 28 d after Immunization with modRNA Encoding RBD V5**

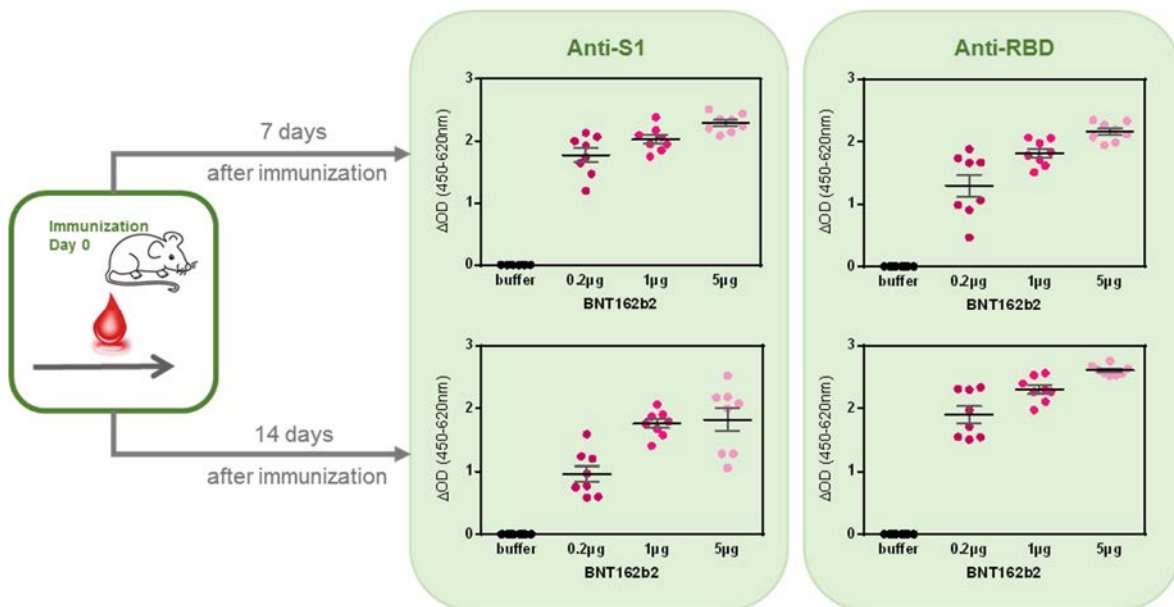


BALB/c mice were immunized IM once with 0.2, 1 or 5 µg of BNT162b1. On 14, 21 and 28 d after immunization, animals were bled, and the sera were tested for SARS CoV-2 pseudovirus neutralization. Graphs depict pVN<sub>50</sub> serum dilutions (50% reduction of infectious events, compared to positive controls without serum). One point in the graphs stands for one mouse. Every mouse sample was measured in duplicate. Group size n=8. Mean ± SEM is shown by horizontal bars with whiskers for each group. LLOQ, lower limit of quantification. ULOQ, upper limit of quantification.

### 2.4.2.1.10.3. Immunogenicity of modRNA Encoding P2 S V9 (BNT162b2/RBP020.2)

The immunogenicity of LNP-formulated modRNA encoding P2S V9 (vaccine candidate BNT162b2) was tested in mice (experimental details in Table 2.4.2-3 and the figure legend). ELISA data show an early, dose-dependent IgG response recognizing S1 and RBD (Figure 2.4.2-24). The study is ongoing. Additional data including neutralization data will be provided before human dosing commences with this candidate.

**Figure 2.4.2-24. IgG Response Recognizing S1 and RBD 7 and 14 d after Immunization with modRNA Encoding P2 S V9**

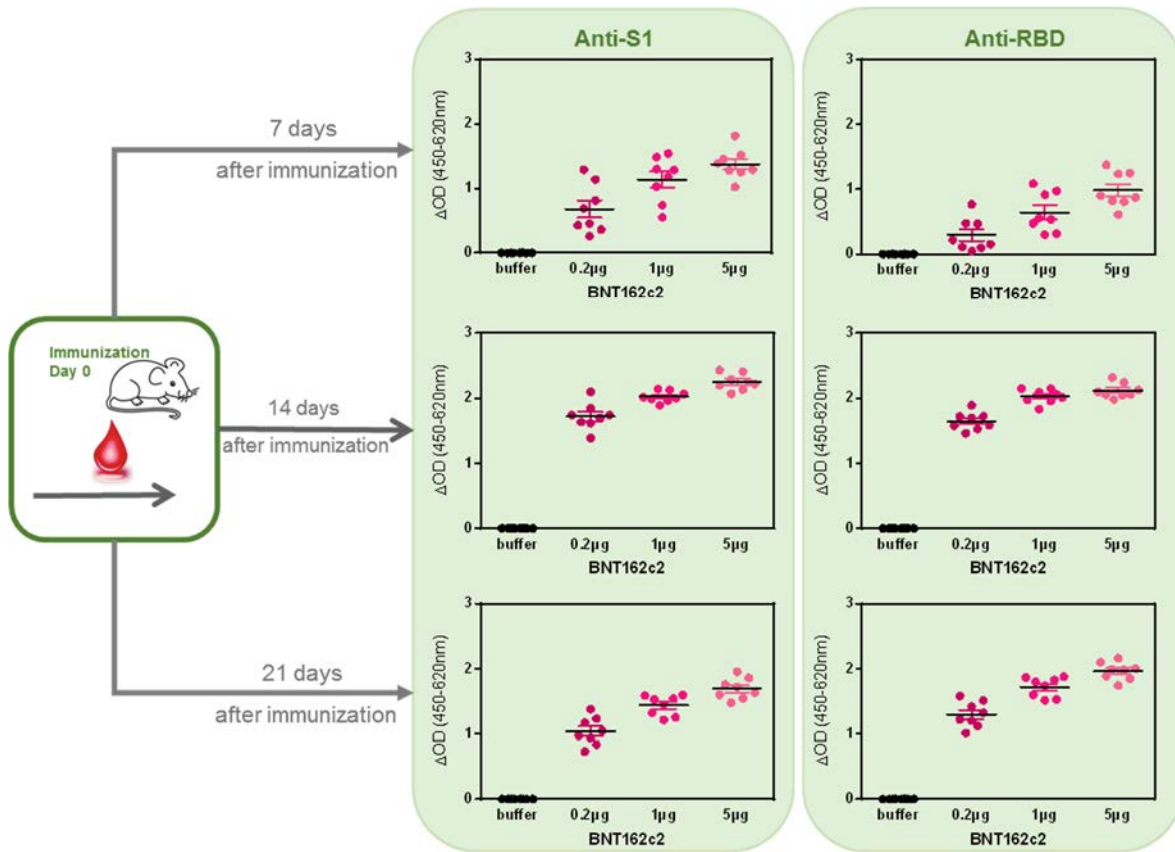


BALB/c mice were immunized IM once with 0.2, 1 or 5 μg of LNP-formulated modRNA vaccine candidate encoding the P2 S-V9 (BNT162b2). On 7 and 14 d after immunization, animals were bled, and the sera were analyzed for anti-S1 (left) and anti-RBD (right) antigen-specific IgG by ELISA. For day 7 (1:300) and day 14 (1:900), data from different serum dilutions were included on the graphs. One point on the graphs stands for one mouse. Every serum sample was measured in duplicate. Group size n=8. Mean ± SEM is depicted by a horizontal line with whiskers for each group.

#### 2.4.2.1.10.4. Immunogenicity of saRNA Encoding P2 S V9 (BNT162c2/RBS004.2)

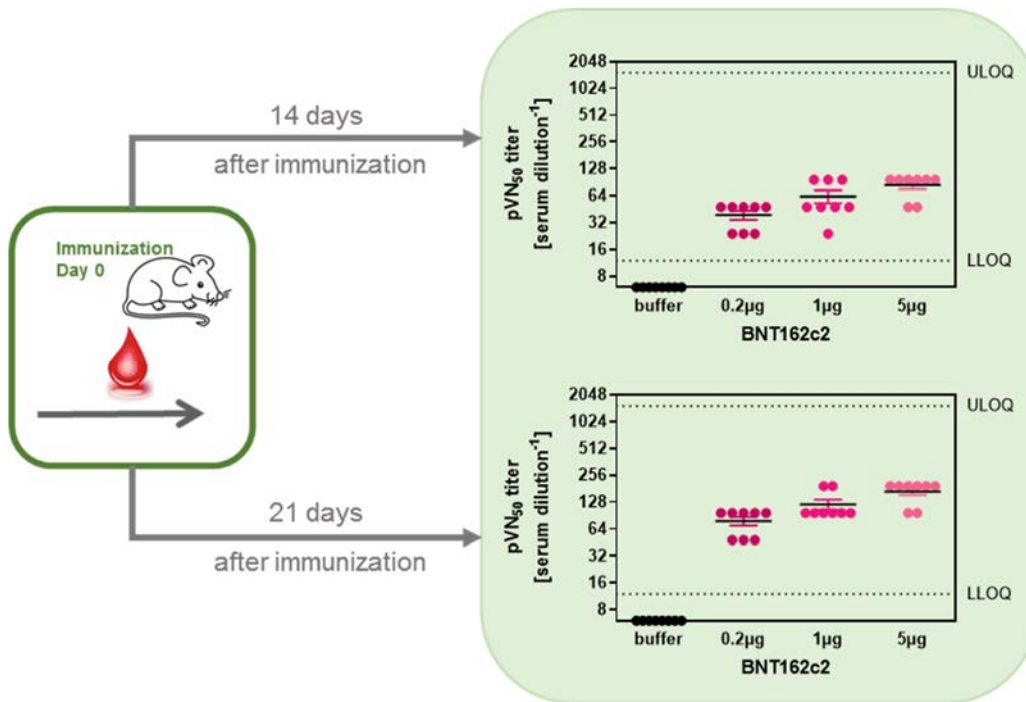
The immunogenicity of LNP-formulated saRNA encoding P2 S V9 (vaccine candidate BNT162c2) was tested in mice (experimental details in Table 2.4.2-3 and the figure legends). ELISA data show an early, dose-dependent IgG response recognizing S1 and RBD (Figure 2.4.2-25). Sera obtained 14 and 21 d after immunization show dose-dependent pseudovirus neutralization (Figure 2.4.2-26). The study is ongoing.

**Figure 2.4.2-25. IgG Response Recognizing S1 and RBD 7, 14 and 21 d after Immunization with saRNA Encoding P2 S V9**



BALB/c mice were immunized IM once with 0.2, 1 or 5 μg of LNP-formulated saRNA vaccine candidate encoding the P2 S-V9 (BNT162c2). 7, 14 and 21 d after immunization, animals were bled and the serum samples were analyzed for total amount of anti-S1 (left) and anti-RBD (right) antigen specific immunoglobulin G (IgG) measured via ELISA. For day 7 (1:100), day 14 (1:300) and day 21 (1:900) different serum dilutions were included in the graph. One point in the graph stands for one mouse, every mouse sample was measured in duplicates (group size n=8; mean ± SEM is included for the groups).

**Figure 2.4.2-26. Pseudovirus Neutralization 14 and 21 d after Immunization with saRNA Encoding P2 S V9**



BALB/c mice were immunized IM once with 0.2, 1 or 5 µg of BNT162c2. On 14, and 21 d after immunization, animals were bled, and the sera were tested for SARS CoV-2 pseudovirus neutralization. Graphs depict pVN<sub>50</sub> serum dilutions (50% reduction of infectious events, compared to positive controls without serum). One point in the graphs stands for one mouse. Every mouse sample was measured in duplicate. Group size n=8. Mean ± SEM is shown by horizontal bars with whiskers for each group. LLOQ, lower limit of quantification. ULOQ, upper limit of quantification.

#### 2.4.2.1.11. Immunogenicity Testing After Weekly Immunization of Rats in the GLP Compliant Repeat Dose Toxicology Study

The immunogenicity of COVID-19 vaccine candidates BNT162a1, BNT162b1, BNT162b2 (RBP020.1), and BNT162c1 in the GLP compliant repeat-dose rat toxicity study (Study 38166) was analyzed. Experimental details are in the figure legends. The rats received two weekly doses of saRNA candidate (BNT162c1) or three weekly doses of the uRNA candidate (BNT162a1) and modRNA candidates (BNT162b1 and BNT162b2/RBP020.1). Serum samples were collected from main study animals on day 10 (BNT162c1) or day 17 (BNT162a1, BNT162b1, and BNT162b2) after the first immunization. These blood draws correspond to 3 days post second dose and 3 days post third dose, respectively.

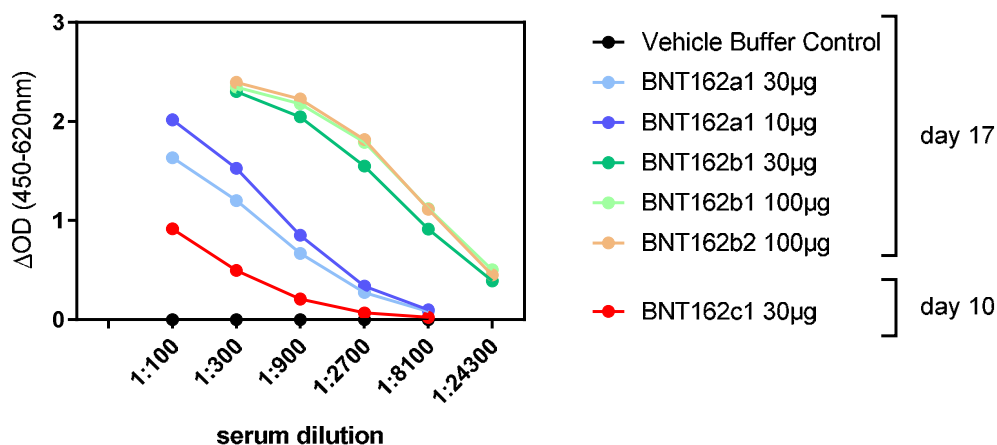
The sera were analyzed by ELISA for IgG that bound S1 (Figure 2.4.2-27) and RBD (Figure 2.4.2-28) and for SARS-CoV2-S pseudovirus neutralization (Figure 2.4.2-29). Each of the vaccine candidates elicited IgG that recognized S1 and RBD. Comparisons between the candidates' immunogenicity are complicated by the differences in dose level and number

of doses, as well timing of blood draws between the RNA platforms and antigens. The rank order of the antigen-binding IgG responses was the same regardless of whether the target antigen in the ELISA was S1 or RBD. The analysis showed the lowest IgG responses to two doses of 30 µg of saRNA encoding the RBD at day 10 after the first immunization, middle IgG responses to three doses of 10 or 30 µg of uRNA encoding the RBD (BNT162a1) at day 17, and the highest antibody responses to three doses of 30 or 100 µg of modRNA encoding RBD (BNT162b1) or of 100 µg of RNA encoding P2 S V8 (BNT162b2/RBP020.1) at day 17. Comparison of the two modRNAs that had the same dosing level and regimen but encoded different antigens (the RBD for B162b1 and P2 S for B162b2/RBP020.1) showed equivalent IgG responses to both target antigens (S1 and RBD) by ELISA.

Antibody concentrations were calculated for the individual serum samples and the concentrations of IgG recognizing S1 and RBD are given in Table 2.4.2-4. Antibody concentrations against S1 and RBD were, as expected, slightly higher for the higher dose of modRNA encoding RBD (BNT162b1) but slightly lower for the higher dose of uRNA expressing RBD (BNT162a1).

Pseudovirus neutralization results paralleled the antigen binding results (Figure 2.4.2-27). The highest neutralizing titers were elicited by three doses of 30 or 100 µg of the modRNAs at day 17, middle neutralizing titers were elicited by three doses of 10 or 30 µg of uRNA at day 17, and minimal to no detectable neutralizing titers were elicited by two doses of 30 µg of saRNA at day 10.

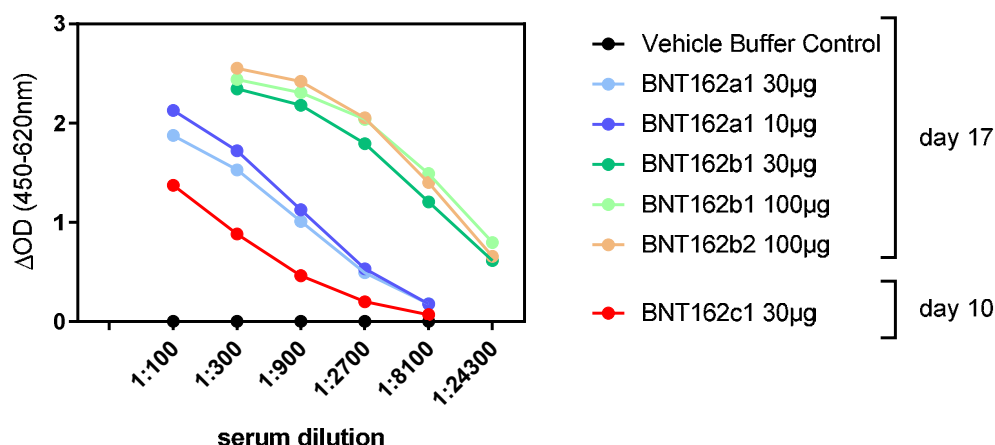
**Figure 2.4.2-27. IgG Responses Recognizing S1 after Repeated Immunization in the Rat Toxicology Study**



Wistar Han rats were immunized IM with three weekly injections of 10 or 30 µg BNT162a1, 30 or 100 µg BNT162b1, 100 µg BNT162b2 (RBP020.1), or two weekly injections of 30 µg BNT162c1. On day 10 (BNT162c1) or day 17 (all other cohorts) animals were bled and the sera were tested for total amount of anti-S1 antigen specific immunoglobulin G (IgG) measured via ELISA. Different serum dilutions were tested ranging from 1:100 to 1:24300. One point in the graph stands for the ΔOD group mean value at a particular given serum dilution (group size n=20).



**Figure 2.4.2-28. IgG Responses Recognizing RBD after Repeated Immunization in the Rat Toxicology Study**



Wistar Han rats were immunized IM with three weekly injections of 10 or 30 μg BNT162a1, 30 or 100 μg BNT162b1, 100 μg BNT162b2 (RBP020.1), or two weekly injections of 30 μg BNT162c1. On day 10 (BNT162c1) or day 17 (all other cohorts) animals were bled and the sera were tested for total amount of anti-RBD antigen specific immunoglobulin G (IgG) measured via ELISA. Different serum dilutions were tested ranging from 1:100 to 1:24300. One point in the graph stands for the ΔOD group mean value at a particular given serum dilution (group size n=20).

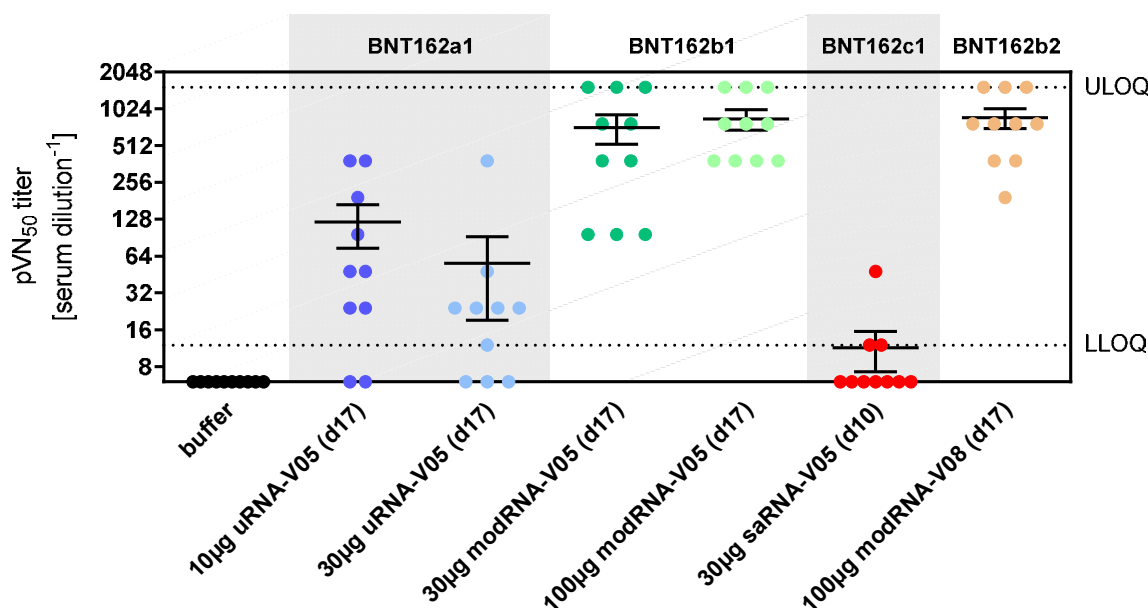
**Table 2.4.2-4. IgG Concentrations Against S1 and RBD in Immunized Wistar Han Rats**

IgG total [μg/mL]	17 d after first immunization					10 d after first immunization
	BNT162a1 30 μg	BNT162a1 10 μg	BNT162b1 100 μg	BNT162b1 30 μg	BNT162b2 100 μg	BNT162c1 30 μg
Against S1	83.0 ± 13.6	149.8 ± 24.6	1844.2 ± 243.4	1502.9 ± 269.9	1755.9 ± 164.1	19.3 ± 3.7
Against RBD	192.6 ± 35.2	208.3 ± 28.9	2632.6 ± 270.9	2017.0 ± 257.1	2331.4 ± 185.1	56.3 ± 12.0

For individual ΔOD values, the antibody concentrations in the serum samples were calculated. The serum samples were tested against the S1 protein and RBD. Group mean antibody concentrations are shown (±SEM) that were graphed in Figure 2.4.2-27 and Figure 2.4.2-28.



**Figure 2.4.2-29. Pseudovirus Neutralization Activity (pVN<sub>50</sub>) in Repeatedly Dosed Rats**



Wistar Han rats were immunized IM with three weekly injections of 10 or 30 µg BNT162a1, 30 or 100 µg BNT162b1, 100 µg BNT162b2 (RBP020.1), or two weekly injections of 30 µg BNT162c1. On day 10 (BNT162c1) or day 17 (all other cohorts) animals were bled and the sera were tested for SARS CoV-2 pseudovirus neutralization. Graphs depict pVN<sub>50</sub> serum dilutions (50% reduction of infectious events, compared to positive controls without serum). One point in the graphs stands for one rat. Every rat sample was measured in duplicate. Group size n=5 male and n=5 female rats. Mean ± SEM is shown by horizontal bars with whiskers for each group. LLOQ, lower limit of quantification. ULOQ, upper limit of quantification.

#### 2.4.2.1.12. Secondary pharmacodynamics

No secondary pharmacodynamics studies were conducted for the COVID-19 vaccine candidates.

#### 2.4.2.1.13. Safety pharmacology

No safety pharmacology studies were conducted as they are not considered necessary according to the WHO guideline (WHO, 2005).

#### 2.4.2.1.14. Nonclinical pharmacology - Conclusions

All nonclinical pharmacology studies and their analysis are ongoing.

The currently available data demonstrate that vaccines based on each of the three RNA platforms (uRNA, modRNA, and saRNA) in conjunction with both the trimerized RBD V5 and P2 S V8 and V9, including the clinical vaccine candidates, BNT162a1, BNT162b1, BNT162b2 (RBP020.1), and BNT162c2, are capable of inducing robust immune responses in mice and rats. In mice, antigen-binding IgG responses were detected as soon as 7 d

post-immunization. Immune responses measured by SARS-CoV-2 pseudovirus neutralization are detectable 14 d post-immunization in mice immunized with intermediate doses. Similar results indicating immunogenicity were obtained in an accessory study to the GLP-compliant repeat-dose toxicology study in rats ([Study 38166](#)).

As both antigen variants, RBD and P2 S, elicit antigen-binding antibodies and pseudovirus-neutralizing serum titers, and all three RNA platforms have proven immunogenic for other viral antigens, these preliminary data support the clinical testing of each of these vaccine candidates.

Differences in results obtained in mice and rats, such as the lack of pseudovirus neutralizing titers elicited in mice ([Section 2.4.2.1.10.1](#)) but robust neutralizing titers elicited in rats ([Section 2.4.2.1.11](#)) by uRNA encoding the RBD, point to complexities in interpretation of results in rodent models. Rather than trying to optimize timing, dose level, and regimen in mice to appropriately describe the immune profiles, which is very time consuming and may not be relevant to the human situation (especially given species-specific innate immune mechanisms), such results provide the rationale for our desire to assess the humoral and cellular immune response to COVID-19 vaccine candidates as quickly as possible in the human sentinel cohorts.

### 2.4.3. PHARMACOKINETICS

#### 2.4.3.1. Brief Summary

Currently, no nonclinical methods of analysis, absorption, PK, TK, metabolism, excretion, or DDI studies have been conducted for the COVID-19 vaccine candidates (BNT162 [PF-07302048]) described in [Section 2.4.1](#).

The biodistribution of the COVID-19 vaccine platform after IM administration was assessed in BALB/c mice. Mice were administered a luciferase expressing modRNA formulated like the COVID-19 vaccine candidates. Luciferase expression was measured in vivo by luciferin application. Luciferase expression was identified at the injection site at 6 hours after injection and was gone by 9 days. Liver expression was also present to a lesser extent at 6 hours after injection and was gone by 48 hours after injection. These data are consistent with the biodistribution that has been observed for RNA platform vaccine candidates that have been already evaluated clinically and have shown a good safety profile (as described in Section 2.4.3.5 below).

#### 2.4.3.2. Methods of Analysis

No nonclinical PK or TK methods of analysis have been developed for the components of the COVID-19 vaccines.

#### 2.4.3.3. In Vitro Absorption

No absorption studies were conducted for the COVID-19 vaccines, as the administration route is IM.

#### 2.4.3.4. Pharmacokinetics

Pharmacokinetic studies have not been conducted with the COVID-19 vaccine candidates and are generally not considered necessary to support the development and licensure of vaccine products for infectious diseases ([WHO, 2005](#); [WHO, 2014](#)).

#### 2.4.3.5. Distribution

To date, whole body distribution studies have not been conducted with the COVID-19 vaccine candidates. In an in vivo study ([Study R-20-0072](#)), the biodistribution was assessed using luciferase as a surrogate marker protein, using RNA encoding luciferase formulated like the COVID-19 vaccine candidates (using LNP8). The RNA was administered to BALB/c mice by IM injection in the right and left hind leg, each with 1 µg of LNP-formulated modRNA encoding luciferase. Luciferase protein expression was detected at different timepoints, by measuring the in vivo bioluminescence after injection of the luciferin substrate, at the site of injection and to a lesser extent in the liver ([Figure 1](#)). Distribution to the liver is likely mediated by the LNPs entering the blood stream. The luciferase expression dropped to background levels after 9 days.

COVID-19 Vaccine (BNT162, PF-07302048)

BB-IND 19736

Module 2.4. Nonclinical Overview

The biodistribution of the antigen encoded by the RNA component of the COVID-19 vaccines is expected to be dependent on the LNP distribution. Therefore, the modRNA encoding luciferase results should be representative for COVID-19 vaccine RNA platforms. BioNTech has safely tested RNAs, formulated in lipoplexes that are similar to LNPs and also show biodistribution to the liver, at higher doses non-clinically and clinically by IV administration. Although liver function tests will be carefully monitored during the clinical development of these vaccines, BioNTech's prior clinical experience indicates that the distribution to the liver does not pose a safety concern. These previous clinical and non-clinical studies conducted by BioNTech are summarized in the included Investigator's Brochure ([April 2020 Investigator's Brochure, Section 2.5 and 4.3.1](#)).

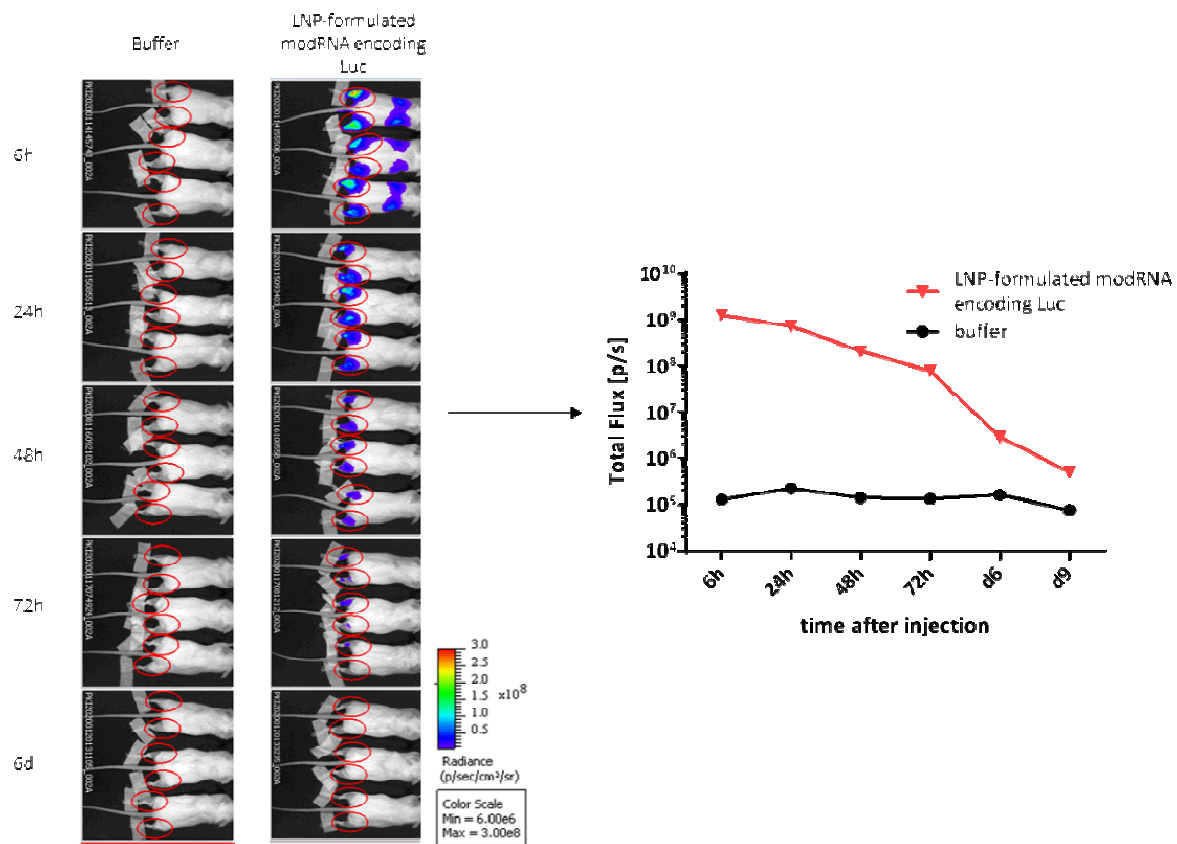


**Figure 1. Bioluminescence Emission in BALB/c Mice after IM Injection of an LNP Formulation of modRNA Encoding Luciferase**

#### 2.4.3.6. Metabolism

Proteins encoded by the RNA in the COVID-19 vaccine candidates are expected to be proteolytically degraded like other endogenous proteins. RNA, including pseudouridine modified RNA and saRNA, is degraded by cellular RNases and subjected to nucleic acid metabolism. Nucleotide metabolism occurs continuously within the cell, with the nucleoside being degraded to waste products and excreted or recycled for nucleotide synthesis.

COVID-19 Vaccine (BNT162, PF-07302048)

BB-IND 19736

Module 2.4. Nonclinical Overview

---

Therefore, no RNA or protein metabolism or excretion studies will be conducted. Of the four lipids used as excipients in the LNP formulation, two are naturally occurring (cholesterol and DSPC) and will be metabolized and excreted like other endogenous lipids. The PK profile of the two novel lipids (ALC-0315 and ALC-0159) will be characterized at a later stage of nonclinical development.

#### **2.4.3.7. Excretion**

No excretion studies have been conducted with the COVID-19 vaccine candidates for the reasons described in [Section 2.4.3.6](#).

#### **2.4.3.8. Pharmacokinetic Drug Interactions**

No PK drug interaction studies have been conducted with the COVID-19 vaccine candidates.

090177e1934a5cff\Approved\Approved On: 21-Apr-2020 19:41 (GMT)

## 2.4.4. TOXICOLOGY

### 2.4.4.1. Brief Summary

A GLP-compliant repeat-dose toxicity study in Wistar Han rats is ongoing to support the nonclinical toxicity assessment of the COVID-19 vaccine candidates (BNT162; PF-07302048) (outlined in [Table 2.4.4-1](#)).

The IM route of exposure was selected as it is the intended route of clinical administration. The selection of rats as the toxicology test species is consistent with the WHO guidance documents on nonclinical evaluation of vaccines ([WHO, 2005](#)), which recommend that vaccine toxicity studies be conducted in a species in which an immune response is induced by the vaccine antigen. Mice have developed an immune response to the COVID-19 vaccine candidates, and immunogenicity has been confirmed in rats in the ongoing repeat-dose toxicity study. The Wistar Han rat is used routinely for regulatory toxicity studies, and there is an extensive historical safety database on this strain of rat.

The non-QC, unaudited interim study report ([Study 38166](#)) includes results of dosing phase mortality, clinical signs, body weight, food consumption, body temperature, injection site dermal scores, ophthalmoscopic and auditory endpoints, hematology, coagulation, clinical chemistry, and urinalysis parameters, a subset of cytokine endpoints, serology, organ weights and macroscopic pathology from dosing phase animals. Remaining cytokine results and microscopic pathology from the dosing phase as well as all the recovery phase endpoints will be submitted in a final report as soon as it becomes available, but no later than 120 days after submission of the IND.

Initial results following administration of COVID-19 vaccine candidates by IM injection to male and female Wistar Han rats once every week, for a total of 2 or 3 weekly cycles of dosing, suggest the COVID-19 vaccine candidates were tolerated without evidence of systemic toxicity.

**Table 2.4.4-1. Overview of Toxicity Testing Program**

Study <sup>a,b</sup>	Dose Group	Dose/Week (µg RNA)	Total Volume (µL)	Tabulated Summary
<b>Repeat-Dose Toxicity</b>				
21-Day, 2 or 3 Dose (1 Dose/Week) <sup>c</sup> IM Toxicity in Rats With a 3-Week Recovery Period (Study 38166)	Control (Buffer <sup>d</sup> )	0	200 (2 x 100 µL) <sup>e</sup>	<a href="#">2.6.7.7A</a>
	BNT162a1 (RBL063.3) (uRNA-LNP RBD V5)	30	60 (1 x 60 µL) <sup>f</sup>	
	BNT162a1 (RBL063.3) (uRNA-LNP RBD V5)	10	20 (1 x 20 µL) <sup>f</sup>	
	BNT162b1 (RBP020.3) (modRNA-LNP RBD V5)	30	60 (1 x 60 µL) <sup>f</sup>	
	BNT162b1 (RBP020.3) (modRNA-LNP RBD V5)	100	200 (2 x 100 µL) <sup>e</sup>	
	BNT162c1 (RBS004.3) (saRNA-LNP RBD V5)	30	70 (1 x 70 µL) <sup>f</sup>	
	BNT162b2 (RBP020.1) (modRNA-LNP SP2 V8)	100	200 (2 x 100 µL) <sup>e</sup>	

a. The repeat-dose toxicity study was GLP-compliant and was conducted in an OECD mutual acceptance of data-compliant member state.

b. The repeat-dose toxicity study was conducted with male and female animals.

c. QW x 3 (Days 1, 8, 15) for BNT162a1, BNT162b1, and BNT162b2; QW x 2 (Days 1, 8) for BNT162c1.

d. Phosphate buffered saline, 300 mM sucrose.

e. One application (100 µL) at 2 sites for a total dose volume of 200 µL.

f. One application at 1 site.

Expected inflammatory responses to the vaccine candidates were evident, such as edema and erythema at the injection sites, transient elevation in body temperature, slight and transient reduction in body weights, elevations in mean neutrophil, monocyte, and LUC counts, and elevations in acute phase reactants. Injection site reactions were common in all vaccine-administered animals and were greater after boost immunizations, which was attributable to the pharmacologically relevant progression of the elicited immune response. Decreased reticulocytes were observed in rats treated with the licensed LNP-siRNA pharmaceutical Onpatro™ (NDA # 210922) but have not been observed in humans treated with this biotherapeutic (Kozauer et al, 2018) suggesting this is a species-specific effect. Decreased platelet counts were noted after repeat administration but based on their small magnitude, no disruptions in hemostasis would be anticipated. Test article-related changes in clinical pathology were consistent with an acute phase response and anticipated low-level systemic inflammation. Macroscopic pathology and organ weight changes were also consistent with an inflammatory response. By the end of the dosing phase, an immune response was elicited from all COVID-19 vaccine candidate groups.



#### 2.4.4.2. Single-Dose Toxicity

A separate single-dose toxicity study with the COVID-19 vaccine candidates has not been conducted.

#### 2.4.4.3. Repeat-Dose Toxicity

##### 2.4.4.3.1. Repeat-Dose Toxicity Study of Three LNP-Formulated RNA Platforms Encoding for Viral Proteins by Repeated Intramuscular Administration to Wistar Han Rats

The objective of this pivotal repeat-dose toxicity study was to determine the potential toxicity of three LNP-formulated RNA vaccine platforms, encoding SARS-CoV-2 P2 S or RBD, administered once weekly by IM administration to rats and to assess the reversibility of any effects after a 3-week recovery period ([Study 38166](#); [Tabulated Summary 2.6.7.7A](#)). The LNP formulation is the same for the three RNA platforms administered in this study.

Wistar Han rats (15/sex/group) were administered COVID-19 vaccine via IM injection at doses of 0 (buffer), 30 and 10 (BNT162a1/RBL063.3), 30 and 100 (BNT162b1/RBP020.3), 30 (BNT162c1/RBS004.3), or 100 (BNT162b2/RBP020.1) µg RNA/dose per animal. Doses were administered once a week for 2 weeks (Days 1, 8) for BNT162c1 or once a week for 3 weeks (Days 1, 8, 15) for BNT162a1, BNT162b1, and BNT162b2. Dose volume ranged from 20 to 100 µL/application site. Following the dosing period, 10 animals/sex from each group were euthanized 2 days post last immunization for post-mortem assessments. The remaining 5 animals/sex/group were euthanized following a 3-week recovery period. Additional satellite animals (3/sex/group) were used for blood sampling for cytokine analysis.

Clinical signs of toxicity were assessed twice daily throughout the study. Body weights were recorded twice weekly during the dosing and the recovery phase. Food consumption was evaluated once weekly. Local tolerance (injection site dermal assessment) was evaluated 4, 24, 48, 96, and 144 hours after each administration, and body temperatures were evaluated at 4 and 24 hours after each administration. Additional body temperature measurements were taken at 48 hours if an animal had a body temperature >40°C. A limited set of serum cytokines (IFN-γ, TNF-α, IL-1-β, IL-6, IL-10) were evaluated prior to and 6 hours post each dose and at the end of the dosing phase. Clinical pathology (hematology and clinical chemistry parameters as well as acute phase proteins) was evaluated 3 days after the first administration and at the end of the dosing and recovery phases. Urine analysis, coagulation parameters, auditory and ophthalmological parameters, serology, organ weights, macroscopic and microscopic pathology were evaluated at the end of dosing and recovery phases.

Interim results from this pivotal repeat-dose toxicity study are summarized below and are also provided in an interim non-QC, unaudited study report ([Study 38166](#)). As agreed with CBER via the Pre-IND Meeting - Request for Written Feedback (Section 1.12.1 Correspondence Regarding Pre-IND Meeting), interim data submitted in this IND include all dosing phase mortality, clinical signs, body weight, food consumption, body temperature, injection site observations, ophthalmoscopic and auditory endpoints, a subset of serum

cytokine endpoints, hematology, coagulation, clinical chemistry, urinalysis parameters, organ weights and macroscopic pathology as well as serology data from animals at the end of the dosing phase. Remaining cytokine results and microscopic pathology from the dosing phase as well as all the recovery phase endpoints will be submitted in a final report as soon as it becomes available, and no later than 120 days after submission of the IND.

At the interim phase of reporting, all test articles were tolerated, and all animals survived to the end of the dosing phase. Test article-related in-life findings included injection site reactions, transient body weight loss the day after dosing, and slightly higher body temperature at 4 and 24 hours postdose.

Body weights decreased 24 hours after each COVID-19 vaccine administration compared to predose values (<10%). No reduction was noted for the buffer control. Body weight gain between the administrations was comparable to the buffer control group.

Vaccine-administered animals generally had higher body temperatures compared to buffer control animals at 4 and 24 hours postdose. Group mean temperatures in COVID-19 vaccine-administered rats were within approximately 1°C of the group mean body temperature of buffer-administered animals. In rare cases, individual COVID-19 vaccine-administered rats had body temperatures up to 40.2°C, which decreased to <40°C within 24 hours after administration.

Slightly lower (0.77x to 0.97x) food consumption was seen in COVID-19 vaccine-administered animals compared to the buffer control group during Week 1, which was not apparent during Week 2.

There were no changes observed in either the ophthalmic or auditory examinations.

Expected inflammatory responses to the vaccine candidates were evident at the injection sites. Injection site reactions consisted primarily of transient edema and erythema, which resolved prior to the subsequent vaccine administration. Injection site reactions were more frequent and severe after the second and third vaccine administrations. The occurrence of higher severity injection site reactions after boost vaccinations is attributable to the pharmacologically relevant progression of the elicited immune response.

After the first vaccine administration, very slight (Grade 1) or slight (Grade 2) edema was noted in some animals across vaccine-administered groups 24 hours post administration. The reaction generally resolved within the following 24 to 48 hours and was resolved in all animals by 144 hours post administration. After the second vaccine administration, the local reaction was more pronounced (Grade 1 to Grade 3 [moderate]) and present in more, though not in all, animals. In animals administered 30 µg BNT162a1, eschar formation at the injection site was apparent for some animals after the second vaccine administration and appeared painful, but resolved. Of note, no Grade 3 or Grade 4 (severe) local reactions occurred after the first administration. The occurrence of higher severity local reactions after the second vaccine administration is attributed to the short dosing interval (once weekly).

090177e1934a5cfaApproved\Approved On: 21-Apr-2020 19:41 (GMT)

Reversible very slight (Grade 1) erythema was noted from 48 to 96 hours post first vaccine administration in some animals in all vaccine-administered groups, except 30 µg BNT162b1.

After the second vaccine administration, very slight (Grade 1) to well-defined (Grade 2) erythema was noted in some animals from 24 to 48 hours (30 µg BNT162a1, 30 µg BNT162b1, 100 µg BNT162b2), and was resolved by 96 hours post administration. However, 144 hours post the second administration, severe (Grade 4) erythema was observed in some vaccine-administered animals (10 µg BNT162a1, 100 µg BNT162b1, 100 µg BNT162b2), but the observation was resolved within the following 24 hours.

Test article-related changes in clinical pathology were consistent with an acute phase response and anticipated systemic inflammation. Minor and variable alterations in other clinical pathology parameters were considered secondary effects of vaccination, including inflammation and injection site tissue changes.

Changes in hematology included lower mean reticulocyte and platelet counts, and higher mean white blood cell, neutrophil, monocyte, and LUC counts compared to control rats.

The transient reduction in reticulocyte counts (0.24x to 0.74x) was only observed after the first dose administration on Day 4 and was not accompanied by a reduction in red blood cell counts or hemoglobin content. Mean reticulocyte decreases were comparable across treatment groups and were likely related to the acute phase response.

Lower platelet counts (0.58x to 0.85x) were observed in all vaccine-administered groups except BNT162b2 at Days 10 or 17 and is likely inflammation-related platelet consumption. These decreases would not be anticipated to result in bleeding based on their small magnitude; there were no clinical findings consistent with disruptions in hemostasis.

Expected inflammatory responses to the vaccine candidates were evident, such as elevations in mean neutrophil (3.7x to 7.8x), monocyte (1.6x to 2.3x), and LUC counts (2.7x to 13x). White blood cells (1.5x to 2.2x) (neutrophils, monocytes, and/or LUC) were higher in all vaccinated groups compared to buffer controls and were higher at Days 10 and 17 than Day 4.

Test article-related changes in clinical chemistry included slightly higher GGT (1.9x to 4.6x) in all treatment groups on Day 4 and Days 10 or 17. This change may be secondary to an inflammatory response ([Singh, 1986](#)).

The acute phase proteins alpha-1-acid glycoprotein (4.1x to 7.2x) and alpha-2 macroglobulin (3.2x to 91x) were elevated in both males and females in all vaccine-administered groups on Day 4. Fibrinogen was higher (2.4x to 3.1x) in both males and females in all vaccine-administered groups on Day 10 or 17. There were no apparent sex related differences in these effects. Higher concentrations of acute phase proteins are an anticipated response to vaccination.

Coagulation parameters PT, aPTT, and fibrinogen were measured at the end of the in-life phase. As noted above, fibrinogen was higher in all vaccine-administered groups

approximately 3X compared to control, consistent with an acute phase response. aPTT was slightly prolonged (up to 1.2x) in all groups except in the 30 µg BNT162b1 group compared to the control group. This increase is likely secondary to inflammation and the low magnitude is not anticipated to cause clinical alterations in hemostasis.

Compared with buffer control, there were no test-article related difference in the concentration of serum cytokines evaluated.

At Days 10 or 17, lower urine volume (as low as 0.67x) and higher urine specific gravity (up to 1.02x) was observed in vaccine-administered groups, likely secondary to dehydration. This correlated with systemic evidence of dehydration in some groups (increases in blood urea nitrogen, creatine, and phosphorus).

Test-article related higher (1.1x to 1.6x) absolute spleen weights were evident in most vaccine administered groups and correlated with the macroscopic observation of increased spleen size. This is likely secondary to immune responses induced by the COVID-19 vaccine candidates.

The most common macroscopic observation in all treatment groups was a thickened injection site and/or induration at the injected muscle. This finding was test-item related and was caused by the local inflammation process. Enlarged spleen and iliac lymph nodes were noted in several animals in the COVID-19 vaccine-administered groups. The effects on the lymphoid organs are consistent with immune responses to the COVID-19 vaccine candidates.

Administration of the vaccine candidates elicited antibody immune responses was evaluated by S1 domain and RBD sub-domain specific ELISA, as well as SARS-CoV-2 S pVNT by Day 10 or 17. The data demonstrates that all COVID-19 vaccine candidates elicited a SARS-CoV-2 S protein specific antibody response directed against the S1 domain and the RBD sub-domain. Antibody responses detected via ELISA directly translated into neutralizing activity as seen in the VSV/SARS-CoV-2 S pVNT. COVID-19 vaccine candidates showing higher antigen-specific antibody titers also displayed more pronounced virus neutralization effect. Additional details on the serology data from Study 38166 are provided in [Section 2.4.2.1.11](#).

In conclusion, administration of COVID-19 vaccine candidates by IM injection to male and female Wistar Han rats once every week, for a total of 2 or 3 weekly cycles of dosing, were tolerated up to 100 µg RNA without evidence of systemic toxicity to any of the COVID-19 vaccine candidates evaluated. Immune responses were generated to all of the vaccine candidates.

#### **2.4.4.4. Genotoxicity**

No genotoxicity studies are planned for the COVID-19 vaccine candidates, as the components of all vaccine constructs are lipids and RNA that are not expected to have genotoxic potential ([WHO, 2005](#)).

090177e1934a5cffApproved\Approved On: 21-Apr-2020 19:41 (GMT)

#### **2.4.4.5. Carcinogenicity**

Carcinogenicity studies with the COVID-19 vaccine candidates have not been conducted as the components of all vaccine constructs are lipids and RNA that are not expected to have carcinogenic or tumorigenic potential. Carcinogenicity testing is generally not considered necessary to support the development and licensure of vaccine products for infectious diseases ([WHO, 2005](#); [WHO, 2014](#)).

#### **2.4.4.6. Reproductive and Developmental Toxicity**

Reproductive or developmental toxicity assessments have not been conducted with the COVID-19 vaccine candidates.

Macroscopic and microscopic evaluation of male and female reproductive tissues will be included in the final report of the pivotal repeat-dose toxicity study ([Study 38166](#)).

#### **2.4.4.7. Local Tolerance**

Local tolerance of IM administration of the COVID-19 vaccine candidates was evaluated by injection site observations, macroscopic, and microscopic examination of injection sites in the pivotal repeat-dose toxicity study and described above ([Section 2.4.4.3.1](#)).

#### **2.4.4.8. Other Toxicity Studies**

##### **2.4.4.8.1. Phototoxicity**

Phototoxicity studies with the COVID-19 vaccine candidates have not been conducted.

##### **2.4.4.8.2. Antigenicity**

Immunogenicity was evaluated as part of the primary pharmacology studies ([Section 2.4.2.1](#)). In general, all three RNA platforms and both antigens generated a robust immune response in non-GLP mouse studies. Interim, serology data from the pivotal repeat-dose toxicity study shows a robust immune response to the COVID-19 vaccine candidates.

##### **2.4.4.8.3. Immunotoxicity**

Stand-alone immunotoxicity studies with the COVID-19 vaccine candidates have not been conducted. However, immunotoxicological endpoints have been collected as part of the pivotal repeat-dose toxicity study.

##### **2.4.4.8.4. Mechanistic Studies**

Mechanistic studies with the COVID-19 vaccine candidates have not been conducted.

**2.4.4.8.5. Dependence**

Dependence studies with the COVID-19 vaccine candidates have not been conducted.

**2.4.4.8.6. Studies on Metabolites**

Stand-alone studies with administration of metabolites of the COVID-19 vaccine candidates have not been conducted.

**2.4.4.8.7. Studies on Impurities**

Stand-alone studies with administration of impurities of the COVID-19 vaccine candidates have not been conducted.

**2.4.4.8.8. Other Studies**

No other studies with the proposed COVID-19 vaccine candidates evaluated in this submission have been conducted.

However, all three RNA platforms have been tested previously using RNAs expressing different genes of interest for other disease targets in several nonclinical GLP safety studies in mice and NHP. These studies have been performed with naked RNAs or RNAs formulated with lipids similar, but not identical, to the lipid nanoparticles to be used in the proposed COVID-19 clinical trial. The nonclinical toxicity data suggest a favorable safety profile for uRNA, modRNA, and saRNA formulated with different lipid vehicles for various administration routes, including IV injection. These studies were conducted by BioNTech and are summarized in the included IB ([Section 4.3.1, Version 3.0, 17 April 2020](#)).

Review of studies conducted with the non-COVID vaccine uRNA in mice and cynomolgus monkeys showed the uRNA/LNP platform to be tolerated. The safety profile of the systemically administered RNA formulation in these studies was characterized by mild findings, which were mostly related to the mode of action and the formulated RNA-intrinsic stimulation of innate immune sensors (eg, transient cytokine increase, hematological changes, and effects on lymphoid organs). IV doses of up to 60 µg/animal of uRNA in mice (Study 28864) and 88.6 µg/animal in cynomolgus monkeys (Study 29928) were tested without any signs of unexpected overstimulation of the immune system.

The data from these studies will not be submitted as part of the IND package as the studies did not use the final clinical candidates and are for background information purposes only.

**2.4.4.9. Target Organ Toxicity**

Based on interim data from the dosing phase of the GLP repeat-dose toxicity study ([Section 2.4.4.3.1](#)), administration of COVID-19 vaccines were associated with local reactogenicity at the injection site and expected acute phase hematological responses. Microscopic findings from this study will be added upon availability.



### 2.4.5. INTEGRATED OVERVIEW AND CONCLUSIONS

The nonclinical program demonstrates that the vaccine candidates are immunogenic in mice and rats, and the toxicity study supports the clinical administration of COVID-19 vaccines up to two (saRNA) or three (uRNA and modRNA) doses at up to 30 µg (uRNA and saRNA) or 100 µg (modRNA). Preclinical assessments in mice demonstrate that COVID-19 vaccine candidates elicit a rapid antibody response that is also functional. Because some mouse studies are still ongoing, additional data will be available prior to human dosing with each vaccine candidate. The data provide proof-of-concept that COVID-19 vaccine candidates can elicit an anti-SARS-CoV-2 immune response and support further investigation of the candidates in humans. Additional characterization of the immune response will be assessed in the ongoing non-human primate immunogenicity study.

The potential biodistribution of the COVID-19 vaccine candidates was assessed using luciferase expression as a surrogate reporter. Protein expression was demonstrated at the site of injection and to a lesser extent in the liver after BALB/c mice received an IM injection of RNA encoding luciferase in a LNP formulation like the COVID-19 vaccine candidates. Luciferase expression was identified at the injection site at 6 hours after injection and was gone by 9 days. Liver expression was also present at 6 hours after injection and was gone by 48 hours after injection consistent with other vaccine candidates that have already been evaluated clinically and shown to be safe.

Based on previous nonclinical and clinical experience with the three RNA platforms, a beneficial safety profile is anticipated, and may include transient local reactions (such as swelling/edema or redness) and body temperature increases. Preliminary data available from the ongoing GLP compliant repeat-dose toxicity study supports this expectation. At the end of the dosing phase, there was no mortality or adverse clinical observations. Transient increases in vaccine-related injection site reactions, inflammatory markers in the blood, and increased body temperature have been observed. These findings are an expected physiological response to an RNA vaccine and were not considered adverse. An immune response to the COVID-19 vaccine candidates was observed at the end of the dosing phase. Given the lack of adverse findings in the interim GLP repeat dose study results, the nonclinical toxicity program supports the clinical administration of COVID-19 vaccines up to 2 (saRNA) or 3 (uRNA and modRNA) doses at up to 30 µg (uRNA, saRNA) or 100 µg (modRNA) per dose.

After initiation of the GLP repeat-dose toxicity study, the decision was made to clinically evaluate BNT162a1 and BNT162b1 in Study C4591001 as planned, but to evaluate 2 alternate vaccine candidates in the place of BNT162b2 (RBP020.1) and BNT162c1 (RBS004.3).

One of the new vaccine candidates for C4591001, BNT162b2 (RBP020.2), encodes P2 S V9. BNT162b2 (RBP020.1), which was tested in the GLP toxicity study, encodes P2 S V8. The 2 antigens, P2 S V8 and P2 S V9, have the same amino acid sequence but different codon optimizations of the antigen's coding sequence. The new codon optimization is anticipated

090177e1934a5cff\Approved\Approved On: 21-Apr-2020 19:41 (GMT)



to increase antigen expression. The new codon optimization is not anticipated to impact the innate response to the RNA.

The other new vaccine candidate for C4591001, BNT162c2 (RBS004.2), is an saRNA-based vaccine candidate that encodes P2 S V9. BNT162c1 (RBS004.3), which is being tested in the ongoing rat GLP repeat dose toxicity study, is an saRNA that encodes the RBD. Both the saRNA platform and P2 S antigen are being evaluated in the ongoing rat GLP repeat-dose toxicity study. These changes are considered to have no safety impact and do not presently require additional toxicity studies to support clinical administration.

Administration of these 2 new vaccine candidates in the clinic is supported by 1) platform safety in multiple GLP toxicity studies and clinical studies with uRNA, modRNA, and saRNA-based vaccines using different lipid vehicles ([Section 2.4.4.8.8](#) and [IB Version 3, 17 April 2020](#)), 2) the interim results of the GLP repeat-dose toxicity study with uRNA (BNT162a1/RBL063.3), modRNA (BNT162b1/RBP020.3 and BNT162b2/RBP020.1), and saRNA (BNT162c1/RBS004.3) candidates, and 3) the similarity of the BNT162b2 variants, with no anticipated changes in safety profile, and 4) in vivo pharmacology studies in rodents showing immunogenicity similar to other candidates and toleration.

Furthermore, the use of these 2 alternative candidates in clinical trials is supported by the 2018 WHO Ebola guidance ([WHO, 2018](#)), which allows for no nonclinical toxicity evaluation with clinical candidates providing adequate nonclinical toxicity testing of the platform, as well as the safety experience with the RNA-LNP platform and ongoing repeat-dose toxicity study with the vaccine antigens.

## 2.4.6. LIST OF LITERATURE REFERENCES

Al-Amri SS, Abbas AT, Siddiq LA, et al. Immunogenicity of candidate MERS-CoV DNA vaccines based on the spike protein. *Sci Rep* 2017;7:44875.

de Wit E, N van Doremalen, D Falzarano, et al. SARS and MERS: Recent insights into emerging coronaviruses. *Nat Rev Microbiol* 2016;14:523-34.

Habibzadeh P, Stoneman EK. The novel coronavirus: a bird's eye view. *Int J Occup Environ Med* 2020;11(2):65-71.

Hulswit RJ, de Haan CA, Bosch B-J. Coronavirus spike protein and tropism changes. *Adv Virus Res* 2016;96:29-57.

Kirchdoerfer RN, Wang N, Pallesen J, et al. Stabilized coronavirus spikes are resistant to conformational changes induced by receptor recognition or proteolysis. *Sci Rep* 2018;8(1):15701.

Kozauer NA, Dunn WH, Unger EF, et al. CBER multi-discipline review of Onpatro. NDA 210922. 10 Aug 2018.

Kranz LM, Diken M, Haas H, et al. Systemic RNA delivery to dendritic cells exploits antiviral defence for cancer immunotherapy. *Nature* 2016;534:396-401.

Moyo N, Vogel AB, Buus S, et al. Efficient induction of T cells against conserved HIV-1 regions by mosaic vaccines delivered as self-amplifying mRNA. *Mol Ther Methods Clin Dev* 2019;12:32-46.

Pallesen J, Wang N, Corbett KS, et al. Immunogenicity and structures of a rationally designed prefusion MERS-CoV spike antigen. *Proc Natl Acad Sci USA* 2017;114(35):E7348-57.

Pardi N, Hogan MJ, Pelc RS, et al. Zika virus protection by a single low-dose nucleoside-modified mRNA vaccination. *Nature* 2017;543(7644):248-51.

Pardi N, Parkhouse K, Kirkpatrick E, et al. Nucleoside-modified mRNA immunization elicits influenza virus hemagglutinin stalk-specific antibodies. *Nat Comm* 2018;9(1):3361.

Pardi N, LaBranche CC, Ferrari G, et al. Characterization of HIV-1 nucleoside-modified mRNA vaccines in rabbits and rhesus macaques. *Mol Ther Nucleic Acids* 2019;15:36-47.

Rauch S, Jasny E, Schmidt KE, et al. New vaccine technologies to combat outbreak situations. *Front Immunol* 2018;9:1963.

Sahin U, Karikó K, Türeci Ö. mRNA-based therapeutics - developing a new class of drugs. *Nat Rev Drug Discov* 2014;13(10):759-80.

COVID-19 Vaccine (BNT162, PF-07302048)

BB-IND 19736

Module 2.4. Nonclinical Overview

---

Singh J, Chander J, Singh S, et al.  $\gamma$ -Glutamyl transpeptidase: a novel biochemical marker in inflammation. *Biochem Pharmacol* 1986;35(21):3753-60.

Study 28864. 6-Week repeated dose toxicity study of RBL001.1, RBL002.2, RBL003.1, and RBL004.1 by intravenous administration to C57BL/6 mice. 11 October 2013. Available upon request.

Study 29928. Pilot pharmacokinetic and pharmacodynamic study of RBL001.1, RBL002.2, RBL003.1 and RBL004.1 after intravenous administration to cynomolgus monkeys.

07 November 2013. Available upon request.

Vogel AB, Lambert L, Kinnear E, et al. Self-amplifying RNA vaccines give equivalent protection against influenza to mRNA vaccines but at much lower doses. *Mol Ther* 2018;26(2):446-55.

World Health Organization. WHO guidelines on nonclinical evaluation of vaccines. Annex 1. In: World Health Organization. WHO technical report series, no. 927. Geneva, Switzerland; World Health Organization; 2005:31-63.

World Health Organization. Annex 2. Guidelines on the nonclinical evaluation of vaccine adjuvants and adjuvanted vaccines. In: WHO technical report series no. 987. Geneva, Switzerland: World Health Organization; 2014: p. 59-100.

WHO Expert Committee on Biological Standardization. Annex 2. Guidelines on the quality, safety and efficacy of Ebola vaccines. In: WHO technical report series, no. 1011. Geneva, Switzerland: World Health Organization; 2018: p. 87-179. Available upon request.

Wrapp D, Wang N, Corbett KS, et al. Cryo-EM structure of the 2019-nCoV spike in the prefusion conformation. *Science* 2020;367(6483):1260-63.

Yong CY, Ong HK, Yeap SK, et al. Recent advances in the vaccine development against middle east respiratory syndrome-coronavirus. *Front Microbiol* 2019;10:1781.

Zakharthouk AN, Sharon C, Satkunarajah M, et al. Immunogenicity of a receptor-binding domain of SARS coronavirus spike protein in mice: implications for a subunit vaccine. *Vaccine* 2007;25(1):136-43.

Zhou M, X Zhang, J Qu et al. Coronavirus disease 2019 (COVID-19): a clinical update. *Front Med* 2020; <https://doi.org/10.1007/s11684-020-0767-8>.

090177e1934a5cff\Approved\Approved On: 21-Apr-2020 19:41 (GMT)